# OIL SPILL DETECTION IN SAR IMAGES USING META-HEURISTIC SEARCH ALGORITHMS

A Thesis

by

SAI VINAY TEJA MANIKONDA

M.S., Texas A & M University - Corpus Christi, 2018

Submitted in Partial Fulfillment of the Requirements for the Degree of

MASTER OF SCIENCE

in

COMPUTER SCIENCE

Texas A&M University-Corpus Christi
Corpus Christi, Texas

May 2018

May 2018

# OIL SPILL DETECTION IN SAR IMAGES USING META-HEURISTIC SEARCH ALGORITHMS

A Thesis

by

SAI VINAY TEJA MANIKONDA

This thesis meets the standards for scope and quality of
Texas A&M University-Corpus Christi and is hereby approved.

Dr. Alaa Sheta
Chair

Dr. Ajay Katangur
Committee Member

Dr. Dulal Kar
Committee Member

May 2018

TABLE OF CONTENTS

CONTENTS PAGE

LIST OF TABLES

TABLES PAGE

LIST OF FIGURES

FIGURES PAGE

# ABSTRACT

In recent years, oil spill accidents have been on rising due to the development of marine transportation and massive oil exploitation. At present, satellite remote sensing is the principal method used to monitor oil spills. Extracting the locations and extent of oil spill spots accurately using remote sensing images reaps significant benefits in terms of risk assessment and clean-up work. Many oil spill detection methods are implemented using traditional K-means and Otsu methods. In this work, traditional segmentation methods K-means and Otsu are improved using Meta- heuristic search algorithms to increase the efficiency of oil spill detection. The Meta-heuristic algorithms used are Genetic Algorithm, Simulated Annealing, and Particle Swarm Optimization. In this work, two frameworks are implemented. Each framework has an image enhancement stage, segmentation stage, and oil extraction stage. The two frameworks differ in the segmentation stage wherein one framework, segmentation is performed based on clustering using Meta-heuristic search algorithms and in the other, segmentation is performed based on thresholding using Meta-heuristic search algorithm. Two fitness functions are developed in this work which will be used for two different frameworks that are afore mentioned. This work is compared to the K-means clustering and Fuzzy c-means algorithm. Segmentation based thresholding using Meta-heuristic Search algorithm with the proposed fitness functions is compared to the Otsu segmentation method.

# CHAPTER 1

# INTRODUCTION

Oil spills are a global concern and oil derivative products are at historic highs for production, transportation, storage, and consumption. In fact statistically, oil and petrochemical spills result in a great damage to marine life. It becomes evident to us that both offshore and onshore spills are of growing public concern [24]. However, innovation of the new methodologies and technologies necessary to protect ourselves and the environment from these sources of oil pollution are being severely outpaced by the growth, demand, and presence of oil. With these premises in mind, the current researchers focus on developing and introducing new remote sensing technology for the prevention, detection, and early warning/containment of oil spills, such as Synthetic Aperture Radar (SAR) [13] and infrared (IR). The on going research in this area shows that there is progress in oil spill detection, although this progress is slow [11]. Furthermore, the efficiency of these technologies is limited due to the noise that may be located on the captured images.

## 1.1 Motivation

Accidental or operational marine oil discharges have a strong impact on the marine wildlife, marine habitats, the economy and the public health [33]. Several methods of clearance and detection were proposed and developed. The most popular method for detection is still manual such as booms and skimmers [21]. These methods are both dangerous and slow. Therefore, there is a need to improve and explore other technologies. Consequently, there is a vast growth sensor technology over the last few years, they require image processing techniques to assist the detection process.

Despite a large number of image processing techniques presently available, there are no general methods, that admits a unique solution. This is due to the variation of the problem and their applications in different fields. The use of any sensor technology [17] requires specific image processing techniques to detect oil spills by using image. Therefore, any sensor-based detection process requires a set of algorithms that extract the features, enhance the image, segment the object and recognize the object as an oil spill or not oil spill. There are several methods for image processing techniques [36], like spatial image processing, wavelet, and morphological image processing. Each of these methods has several algorithms to process the image and filter out the noise. The selection of these algorithms strongly influences the effectiveness and performance of the detection process. It was stated that general solutions are not possible and each sensor technology has its own solution. In brief, detecting an oil spill in the image is a problem with high complexity [12].

Most of which have been developed with a certain class of the image or sensor technology. Development of an automated system for oil spill detection process is based on the combination of sensor technologies and image processing techniques which remains an open problem and an active research area of interest.

## 1.2 Objective

Thesis objectives can be summarized as follows :

The main objective of this work is to create an efficient process for Oil spill detection using Meta-heuristic search algorithms using two models:

- Segmentation based on clustering using Meta-heuristic search algorithms
- Segmentation based on OTSU Multilevel thresholding using Meta-heuristic

search algorithms

# CHAPTER 2

## PROBLEM OF OIL SPILL DETECTION

Oil has long been used as a source of heat and light, but with the advent and innovations in automobile technology, it has become a source of power for transport. Developments in petrochemical industry warrants increased oil supply carried through pipelines and ships from places where it is found to the most convenient sites for refineries and chemical manufacturing plants. The quantity of oil moved by marine transport has enormously increased in volume encompassing tankers with capacity ranging from 100,000 to 500,000 tones resulting in increased possibility of its spillage by accidents or due to operations. The larger the ships the greater will be the volume of oil that would be spilled in the event of an accident. Hence, oil pollution will be encountered in a marine environment or in inland water by fuel cargo containers [7].

Petroleum products play an important role in modern society, particularly in the transportation, plastics, and fertilizer industries. There are typically ten to fifteen transfers involved in moving oil from the oil field to the final consumer. Oil spills can occur during oil transportation or storage and spillage can occur in water, ice or on land. Marine oil spills can be highly dangerous since wind, waves, and currents can scatter a large oil spill over a wide area within a few hours in the open sea. Between 1988 and 2000, there were 2,475 spills which released over 800,000 liters of oil in Toronto and surrounding regions. Environmental rules, regulations and strict operating procedures have been imposed to prevent oil spills, but these measures cannot completely eliminate the risk [17].

The major source of oil pollution is due to the following:

1. Tanker accidents: Large tankers carrying oil over the sea result in the possibility of greater oil spillage in the event of an accident.

2. Ballast water: When unloaded, returning tankers take on seawater as ballast to be carried in the compartments previously occupied by oil. The walls of the compartments are cleaned of clinging oil by powerful jets of seawater. Hence, ballast water inevitably acquires a considerable quantity of oil, which when discharged causes unacceptable oil spill pollution.

Once the oil is spilled, it quickly spreads to form a thin layer on the water surface, known as an "oil slick" [10]. As time passes, the oil slick becomes thinner, forming a layer called "sheen" which has a rainbow-like appearance. Light oils are highly toxic but evaporate quickly. Heavy oils are less toxic but persist in the environment for a long time. Heavy oils can get mixed with pebbles and sandy beaches where they may remain for years. Worldwide, fuels account for 48% of the total oil spilled into the sea worldwide, while crude oil spills account for 29% of the total. The environmental impacts of oil spills can be considerable [17]. Oil spills in water may severely affect the marine environment causing a decline in phytoplankton and other aquatic organisms. Phytoplankton is at the bottom of the food chain and can pass absorbed oil on to higher levels in the food chain. Oiled birds suffer from behavioral changes and may result in the loss of eggs or even death. The livelihood of many coastal people can be impacted by oil spills, particularly those whose livelihood is based on fishing and tourism. The movement of oil on land depends on various factors such as the type of oil, soil type and moisture content of the soil. Oil spilled on agricultural land can impact soil fertility and pollute groundwater resources [17].

## 2.1 What is an Oil Spill?

An oil spill is the release of a liquid petroleum hydrocarbon into the environment due to human activity and is a form of pollution. The term often refers to marine oil spills, where oil is released into the ocean or coastal waters. The oil may be a variety of materials, including crude oil, refined petroleum products (such as gasoline or diesel fuel) or by-products, ship bunkers, oily refuse or oil mixed in waste. Spills take months or even years to clean up. Oil is also released into the environment from natural geologic seeps on the seafloor. Most man-made oil pollution comes from land-based activity, but public attention and regulation have tended to focus most sharply on seagoing oil tankers.

An oil spill is oil discharged accidentally or intentionally, that floats on the surface of water bodies as a discrete mass and is carried by the wind, currents, and tides. Oil spills can be partially controlled by chemical dispersion, combustion, mechanical containment, and adsorption. They have destructive effects on coastal ecosystems.

## 2.2 Behavior of Spilled Oil

To understand the fundamental problems that continue to defy a simple technological solution to oil spills it is necessary to examine some of the main factors that determine the seriousness of a spill, before examining the limitations of the cleanup techniques that are currently available.

## 2.3 Oil Movement

When the oil is spilled onto the surface of the sea it spreads very rapidly, and after a few hours, the slick will usually also begin to break up and form narrow bands or "windrows" parallel to the wind direction. Within a very short time, the oil will often be scattered within an area of many square miles with large variations in oil thickness being evident. This is one of the fundamental factors that limit the effectiveness of all-at-sea response techniques.

Whilst computer models can be used to calculate the probable movement and spreading of spilled oil, experience shows that it is unwise to place total reliance on such predictions. Inadequate knowledge of surface currents in the area of the spill, local wind variations and the unpredictable behavior of some oils (e.g. submergence of heavy oils in rough seas or low salinity waters due to neutral buoyancy) are among the factors that can cause spilled oil to move in surprising directions. This is why aerial surveillance by experienced observers, possibly supplemented by remote sensing equipment if available, is an essential element of an effective response. Surveillance flights should be undertaken at the outset of an incident and then on a regular basis thereafter to confirm the location and extent of the pollution and to verify and update predictions on the oil's probable movement and the threat it poses to sensitive resources [38]. It is important to coordinate flights and flight plans to avoid duplication and to prevent unnecessary disturbance of colonies of seabirds and marine mammals, which might otherwise be frightened into diving into nearby floating oil.

Regrettably, experience shows that aerial surveillance following spills is often inadequate, with common problems including the use of inappropriate aircraft (e.g. jet fighters) and inexperienced observers who are unable to distinguish between thin sheens, thick oil, mousse and a variety of other phenomena that can look like oil

from the air (e.g. underwater seagrass beds). A further very common problem is a failure to transmit clear reports on oil location and reliable estimates of an amount to the control center in a timely manner.

## 2.4 Weathering

At the same time as the oil spreads moves and fragments, it also undergoes a number of physical and chemical changes, collectively termed weathering. Most of these weathering processes, such as evaporation, dispersion, dissolution, and sedimentation, lead to the disappearance of oil from the sea surface. On the other hand, the formation of the water-in-oil emulsion ("mousse") and the accompanying increase in viscosity as the oil absorbs up to four times its own volume of water, promote the oil's persistence. Ultimately, the marine environment assimilates split oil through the long-term process of biodegradation [23].

The speed and relative importance of the processes depends on factors such as the quantity and type of oil, the prevailing weather and sea conditions, and whether or not the oil remains at sea or is washed ashore. An understanding of these interacting factors and processes is essential in order to determine the seriousness of a spill and he needs for a cleanup response.

## 2.5 Type of Oil

One of the most significant factors in any spill is the type of oil, especially its probable persistence in the marine environment.

In general, non-persistent oils include light refined products (e.g. gasoline) and even some light crude oils which are highly volatile materials with low viscosities. As they do not normally persist on the sea surface for any significant time due to

rapid evaporation and the ease with which they disperse and dissipate naturally there is usually only a limited requirement for cleanup. Such oils may, however, pose a significant fire and explosion hazard as well as cause public health concerns if they occur close to centers of population. They may also cause significant environmental impacts due to their high concentration of toxic components but, as these same components evaporate rapidly, any such effects will usually be highly localized.

At the other end of the spectrum of oil, types are heavy crude and heavy fuel oils. These oils are highly persistent when spilled due to their greater proportion of non-volatile components and high viscosity. Such oils have the potential, therefore, to travel great distances from the original spill location, causing widespread contamination of coastlines and damage to amenity areas, fishing gear, and wildlife, mainly through physical smothering. As a consequence, the cleanup of heavy oil spills can be extremely difficult, extend over large areas and be costly. This is well illustrated by the recent ERIKA and NAKHODKA spills in France and Japan, respectively. It is also demonstrated by the TANIO, which broke up off the north coast of Brittany, France in 1980. In this case, the cleanup of the 14,500 tones of heavy fuel oil cargo that contaminated over 200 km of the Brittany coastline was in many ways just as difficult as for the 223,000 tones of crude oil from the AMOCO CADIZ which had contaminated the same area two years earlier. The problem of dealing with heavy oils is also the reason why bunker spills from non-tankers can often cause problems that are far greater than might be suggested by the amount of oil spilled.

Between the two extremes of gasoline and heavy fuel oil there are many intermediate crude oils and refined products that are transported by tankers and used in a variety of marine engines. It is therefore important when a spill occurs to know the exact type of oil involved and its characteristics. This can sometimes be difficult

to determine with certainty during the early stages of a spill, leading to confusion and unreliable predictions.

## 2.6 Methods of Clean up the Spilled Oil

A sheen is usually dispersed (but not cleaned up) with detergents which make oil settle to the bottom. Oils that are denser than water, such as Polychlorinated biphenyls (PCBs), can be more difficult to clean as they make the seabed toxic. In the following sections, we will describe briefly the methods for cleaning the spilled oil.

### 2.6.1 Manual Recovery

Figure 2.1 shows how manual recovery works to clean the oil spill[34].

**Figure 2.1.** Agents manually recovering oil spilled

### 2.6.2 Booms

Booms [39] are large floating barriers that round up oil and lift the oil off the water as shown in Figure 2.2.

**Figure 2.2.** The floating devices are called booms

### 2.6.3 Skimmers

A skimmer is a machine that separates a liquid or particles floating on another liquid as shown in Figure 2.3. A common application is removing oil floating on water. These technologies are commonly used for oil spill remediation but are also commonly found in industry [6].

**Figure 2.3.** Skimmer used to remove spilled oil

### 2.6.4 Sorbents

Sorbets [8] are materials that recover oil by absorption/adsorption as shown in Figure 2.4.

### 2.6.5 Burning

This technique involves controlled burning of the oil at or near the spill site [1].

**Figure 2.4.** The white materials are sorbents

# CHAPTER 3

# IMAGE ENHANCEMENT AND SEGMENTATION

There are several image enhancement techniques, depending on the image and application [4]. Each oil spill detection site uses specific image processing techniques. In general at the acquisition time the contrast is low and the noise is dominant over the image. The contrast enhancement and noise reduction techniques in addition to segmentation are required to detect the spilled oil using images. Consequently, there is a general sequence of processes required to detect the spilled oil using images. Figure 5.1 shows the system design for processing the oil spill images. We will explore each component of this design in details in the following sections. Before that, we will review some basic concepts about the spatial domain.

## 3.1 Basic Concepts of Spatial Domain

Spatial domain refers to the aggregate of pixels composing an image [2]. Spatial domain methods are procedures that operate directly on these pixels. Spatial domain processes can be denoted by the following equation.

$$g(x, y) = T[f(x, y)] \tag{3.1}$$

where $f(x, y)$ is the input image, $g(x, y)$ is the processed image, and $T$ is an operator on $f$, defined over some neighborhood of $(x, y)$.

### 3.1.1 Filters

When the values of f in a predefined neighborhood of $(x, y)$ determine the value of $g$ at $(x, y)$. This is achieved through the use of filters (or kernels, templates, or

windows, or masks) [22]. The values in a filter are referred to as coefficients, rather than pixels. Usually it is deformed by using a 3×3 matrix as shown in the equation 3.2.

$$\begin{pmatrix} C1 & C2 & C3 \\ C4 & C5 & C6 \\ C7 & C8 & C9 \end{pmatrix} \tag{3.2}$$

## 3.2 Image Enhancement

Contrast is referred as the difference in gray levels or luminance values over some areas of the image. Low contrast images can result from poor illumination, lack of dynamic range in the imaging sensor, or even incorrect setting of a lens aperture during image acquisition. There are several techniques such as low power transformation, contrast stretching, histogram equalization, gray level slicing, histogram equalization and image multiplication [30].

### 3.2.1 Contrast Stretching

Contrast stretching is a simple image enhancement technique that attempts to improve the contrast in an image by stretching the range of intensity values it contains to span the desired range of values, e.g. the full range of pixel values that the image type allows. The idea behind it is to increase the dynamic range of the gray levels in the image being processed [28]. So, in this type of transformation is used to enhance low contrast images. In a low contrast image, specific details are difficult to determine due to the fact that most pixels are at the same intensity value. Contrast stretching resolves this problem by boosting the lighter pixels to a higher intensity

level and doing exactly the opposite to the lower intensity pixels.

$$s = T(r) = \frac{1}{1 + (m/r)^E} \tag{3.3}$$

Where $r$ represents the intensities of the input image, $s$ the corresponding intensities values of the output image and $E$ controls the slope of the function.

## 3.3 Image Clustering

Clustering is an important unsupervised classification technique where a set of patterns, usual vectors in a multi-dimensional space, are grouped into clusters in such a way that patterns in the same cluster are similar in some sense and patterns in different clusters are dissimilar in the same sense. For this, it is necessary to first define a measure of similarity which will establish a rule for assigning patterns to the domain of a particular cluster center. One such measure of similarity may be the Euclidean distance $D$ between two patterns $x$ and $z$ defined by $D = ||x - z||$. Smaller the distance between $x$ and $z$, greater is the similarity between the two and vice versa. The final clustering result can depend on the selection of initial centroids, so a lot of thought has been given to this problem.

### 3.3.1 K-means clustering

K-means clustering is done by selecting k points as starting centroids (centers of clusters) [26]. We can just select any k random points, or we can use some other approach, but picking random points is a good start. Then, we iteratively repeat two steps:

- Assignment step: each of the points from the dataset is assigned to a cluster that is represented by the closest of the k centroids. For each point, we calculate

distances to each centroid, and choose that are within the least distance.

- Update step: for each cluster, a new centroid is calculated as the mean of all points in the cluster [29]. From the previous step, we have a set of points which are assigned to a cluster. Now, for each such set, we calculate a mean that we declare as new centroid of the cluster.

After each iteration, the centroids converge, and the total distance from each point to its assigned centroid gets lower and lower. The two steps are alternated until convergence, meaning until there are no more changes in cluster assignment. After a number of iterations, the same set of points will be assigned to each centroid, therefore leading to the same centroids again. K-Means is guaranteed to converge to a local optimum. However, this does not necessarily have to be the best overall solution (global optimum).

One simple solution is to run K-Means a couple of times with random initial assignments. We can then select the best result by taking the one with the minimal sum of distances from each point to its cluster the error value that we are trying to minimize in the first place.

### 3.3.2 Fuzzy C-means Clustering

Fuzzy C-means (FCM) is a method of clustering which allows one piece of data to belong to two or more clusters. This method (developed by Dunn in 1973 and improved by Bezdek in 1981) [9] [32] frequently used in pattern recognition. It is based on minimization objective function as shown in Equation 3.4:

$$j_{im} = \sum_{i=1}^{N} \sum_{j=1}^{C} u_{ij}^{m} ||x_i - c_j||^2, 1 \leq m < \infty \tag{3.4}$$

where m is any real number greater than 1, $u_{ij}$ is the degree of membership of $x_i$ in the cluster $j$, $x_i$ is the ith of d-dimensional measured data, $c_j$ is the d-dimension center of the cluster, and $||*||$ is any norm expressing the similarity between any measured data and the center.

## 3.4 Image Segmentation

Image segmentation consists of finding the shape of objects in different types of images. The main goals of image segmentation are to obtain an automatic segmentation algorithm that can segment an image into its constituent regions or objects. The level to which the subdivision is carried depends on the problem being solved. There are several algorithms for image segmentation.

### 3.4.1 What is Thresholding?

Image thresholding is an important step in many image processing applications. It can be used as a separate block or as a preprocessing step in applications such as Object Character Recognition (OCR) [14]. Segmentation or thresholding is basically dividing the image into several objects is such a way that similar pixels are grouped together in on segment [30]. Although a number of image thresholding techniques are available now, image thresholding is still a challenging problem and they're not yet an optimal technique that can always produce acceptable results with all type of images. We will discuss thresholding technique as a simple and popular method used for segmentation. The thresholding can be performed by using the histogram of the images, where we can clearly find the difference among the threshold values. Here we find the threshold values where the difference between the two segments will be high. Using these threshold values the image can be segmented. In an ideal case,

the histogram has a deep valley between two peaks that represent the objects and background, respectively. The gray-level value at the bottom of the valley can be chosen as the threshold, which is obtained from. In other words suppose there is an image $f(x, y)$, composed of light objects on a dark background, one obvious way to extract the objects from the background is to select a threshold T that separates the object from its background. Then any point $(x, y)$ for which $f(x, y) > T$ is called a point object; otherwise, the point is called a background point.

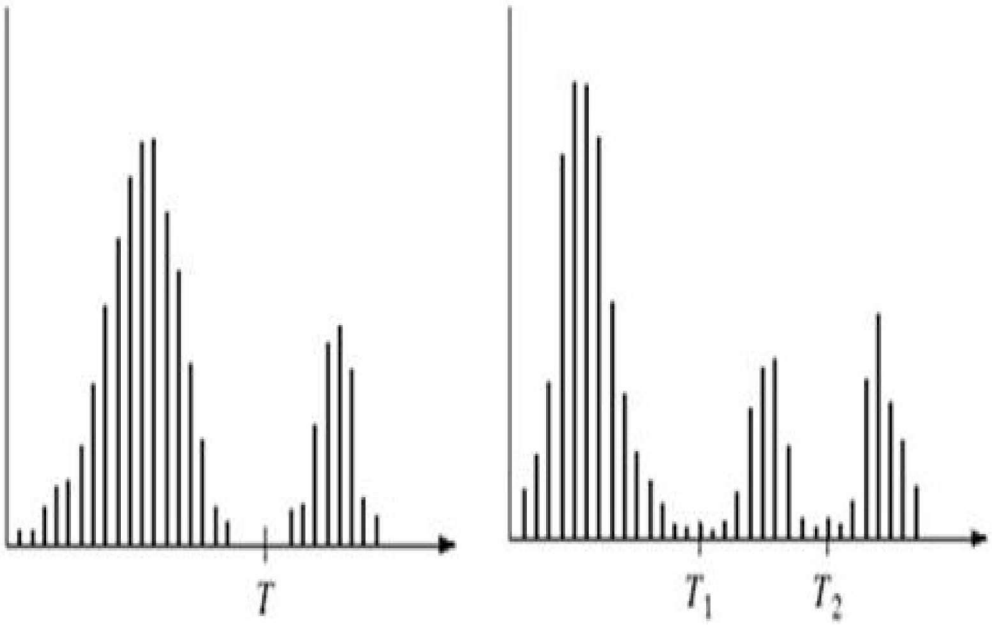


**Figure 3.1.** Single and multiple thresholding: a) Gray level histogram can be partitioned by a single threshold $T$ b) multiple threshold $T_1$ and $T_2$

$$g(x, y) = \begin{cases} 0, iff(x, y) > T \\ 1, iff(x, y) <= T \end{cases} \tag{3.5}$$

In the other case; suppose there are three dominant characterize the image histogram. Here, multilevel thresholding classifies a point$(x, y)$ as belonging to one object class if $T_1 <(x, y)\ T_2$, and to other object class if $f(x, y) > T_2$, and to the background if $f(x, y) < T_2$. We conclude from the above statements that, thresholding may be viewed as an operation that comprises tests against function T of the form shown in the equation 3.5.

$$T = T[x, y, p(x, y), f(x, y)] \tag{3.6}$$

Where $f(x, y)$ is the gray level of point $(x, y)$ and $p(x, y)$ represents some local property of this point, the average gray level of a neighborhood centered on $(x, y)$. When $T$ depends only on $f(x, y)$ that is in the gray level values, the threshold is called "global". If $T$ depends on both $f(x, y)$ and $p(x, y)$, the threshold is called "local".

### 3.4.2 Thresholding Using Otsu Method

The Otsu based between-class variance algorithm can be described as follows:

If an image can be divided into two classes, $C_0$ and $C_1$, based on a threshold at a level $t$, class $C_0$ contains the gray levels from values 0 to $t-1$ and class $C_1$ consists of the other gray levels with values $t$ to $L-1$ [37]. The gray level probabilities and distributions for the two classes are as follows:

$$C_0 : \frac{P_0}{w_0} ... \frac{P_{t-1}}{w_0} \quad C_1 : \frac{P_t}{w_1} ... \frac{P_{L-1}}{w_1} \tag{3.7}$$

where $w_0 = \sum_{t=1}^{t-1} P_t$ and $w_1 = \sum_{i=t}^{L-1} P_t$

Mean levels $\mu_0$ and $\mu_1$ for classes $C_0$ and $C_1$ are as follows:

$$\mu_0 = \sum_{i=0}^{t-1} \frac{iP_t}{w_0}, \quad \mu_1 = \sum_{i=t}^{L-1} \frac{iP_t}{w_1} \tag{3.8}$$

Let $\mu_T$ be the mean intensity for the whole image, it is easy to show that

$$w_0\mu_o + w_1\mu_1 = \mu_T \quad and \quad w_0 + w_1 = 1 \tag{3.9}$$

Using discriminant analysis, Otsu between-class variance thresholded image can be defined as follows:

$$f(t) = \sigma_0 + \sigma_1 \tag{3.10}$$

where $\sigma_0 = w_0(\mu_0 - \mu_T)^2$ and $\sigma_1 = w_1(\mu_1 - \mu_T)^2$

For bi-level thresholding, Otsu selects an optimal threshold $t_1$ and $t_2$ that minimizes the sum of intra class variance. The intra class variance is calculated for two threshold values and the lease sum is chosen as the best intra class variance and the threshold values will be used to segment the image.

# CHAPTER 4

# META-HEURISTIC SEARCH ALGORITHMS

In this chapter, we introduce three different meta-heuristic search algorithms used in this work. They are the Genetic Algorithm (GA), Simulated Annealing (SA) and Particle Swarm Optimization (PSO).

## 4.1 Genetic Algorithm

GA is an evolutionary approach, which applies evolutionary operators and a population of solutions to achieve a globally optimal solution. GA include selection, recombination, and mutation. Candidate solutions to the problem are encoded as chromosomes, and then a fitness function inversely proportional to the mean squared error value is applied to determine the chromosomes surviving likelihood in the next generation. In GA we use a model of the natural selection in real life, where an initial population of solutions called individuals is randomly generated. The algorithm produces new solutions of the population by genetic operations, such as reproduction, crossover and mutation [5]. The new generation consists of the possible survivors with the highest fitness score, and new individuals estimated from the previous population using the genetic operations.

GA searches the solution space of a function through the use of simulated evolution, i.e., the survival of the fittest strategy [15]. GA was used to solve linear and nonlinear problems by exploring all regions of the state space and exponentially exploiting promising areas through mutation, crossover, and selection operations applied to individuals in the population. Which are individual solutions (analogous to chromosomes) of the state space? These operators, which rely on probability rules,

are applied to the population, and successive generations are produced.

In general, the starting search for an optimal solution begins with a randomly generated population of chromosomes. Each generation will have a new set of chromosomes obtained from the application of the operators. A fitness, or objective function, is defined according to the problem. The parent selection process ensures that the fittest members of the population have the highest probability of becoming parents, in the hope that their offspring will combine desirable features, and have superior fitness, to both. The algorithm terminates either when a set of generation number is reached, or the fitness has reached a "satisfactory" level. The use of a GA requires the determination of six fundamental issues:

1. Representation
2. Distribution of initial population
3. Fitness Function
4. Selection Mechanism
5. Reproduction Parameters (i.e., Crossover and Mutation)
6. Termination Criteria

The main steps for GA procedure can be summarized as follows:

1. Generate an initial population.
2. Evaluate the fitness of each individual according to the given fitness function.
3. Select the fittest individual for mating.
4. Apply reproductive operators (e.g. crossover, mutation) to create offspring.

5. Evaluate the fitness of the offspring and select the fit individuals from the current generation and the offspring. They form the population of the next generation.

6. Stop if the stopping criterion is met, else go to step 3.

The GA can be presented as in Figure 4.1.

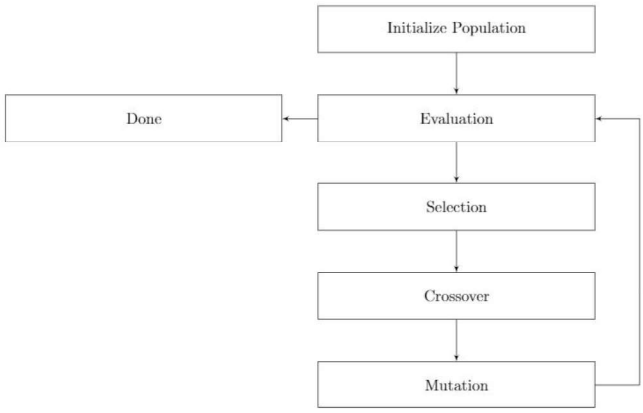


**Figure 4.1.** GA process flow

## 4.2 Simulated Annealing

SA [20] is a stochastic optimization technique introduced by Kirkpatrick. This algorithm begins by selecting an initial solution and later generating a new state, randomly generating a new solution in the neighborhood of the current solution; this is called a neighbor solution [31]. This new state is evaluated and compared with the previous solution. If the solution from the new state is better than the previous one, it is accepted; but if it is not, it is accepted or rejected with some probability. The probability of accepting a new state is given by:

$$P^{(e^{-\Delta E/T})} > R \tag{4.1}$$

$\Delta$E: Difference between the present and the candidate solutions T: Temperature R: a Random uniform number between [0,1] $\Delta$E reflects the change in the objective function and T is the current temperature. The way the temperature decreases as the algorithm is commonly known as the Cooling Schedule and several types of cooling can be found in the literature as well as stopping criterion of the algorithm [25].

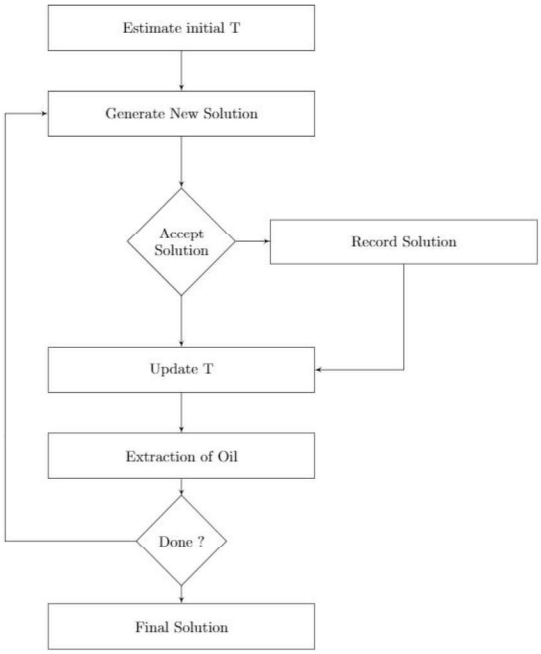


**Figure 4.2.** SA process flow

At each step of the SA algorithm a random nearby state $X_{i+1}$ is generated from the current system state $X_i$. A downhill move (a state with lower energy) is always accepted, an uphill move is accepted with a probability $p(\Delta E, T)$ that depends on the energy difference between the states and on a global parameter $T$, serving as

a fictitious temperature that is gradually decreased during the process [3]. The dependency of the parameters are such that the current solution changes almost randomly when $T$ is high but increasingly goes downhill as $T$ goes to zero. The allowance for uphill prevents the method from becoming stuck at local minima. For accepting or rejecting uphill trial moves we use the standard Metropolis criterion given by

$$p(\Delta E, T) = e^{-\Delta E/cT} \tag{4.2}$$

where c is a constant.

The above is a general description of the SA algorithm. For our goal, segmentation by SA, two decisions have to be made: how to generate a new state and what annealing (cooling) schedule to use.

## 4.3 Particle Swarm Optimization

PSO belongs to a class of swarm intelligence techniques that are used to solve optimization problems [3].Each particle in PSO is updated by following two "best" values:

- *pbest*- Each particle keeps track of its coordinates in the solution space which is associated with the best solution (i.e fitness) that has achieved so far by that particle. This value is called personal best, *pbest*.

- *gbest*- It is tracked by the PSO is the best value obtained so far by any particle in the neighborhood of that particle. This value is called Global Best, *gbest*.

The PSO Algorithm works as follows:

Let X and V denote the particles position and its corresponding velocity in search space respectively. At iteration K, each particle i has its position defined by $X_i^K = [X_{i,1}, X_{i,2}, ...., X_{i,N}]$ and a velocity is defined as $V_i^K = [V_{i,1}, V_{i,2}, ...., V_{i,N}]$ in search space N. Velocity and position of each particle in the next iteration can be calculated as shown in Equation 4.3.

$$V_{i,n}^{k+1} = W * V_{i,n}^k + C_1 * rand_1 * (pbest_{i,n} - X_{i,n}^k) + C_2 * rand_2 * (gbest_n - X_{i,n}^k) \quad (4.3)$$

$$where i = 1, 2.....m \quad and \quad n = 1, 2.....N$$

$$X_{i,n}^{k+1} = \begin{cases} X_{i,n}^k + V_{i,n}^{k+1}, & if X_{min,i,n} <= X_i^{k+1} <= X_{max,i,n} \\ X_{min,i,n}, & if X_i^{k+1} < X_{min,i,n} \\ X_{max,i,n}, & if X_i^{k+1} > X_{max,i,n} \end{cases} \quad (4.4)$$

The inertia weight W is an important factor for the PSO convergence. It is used to control the impact of the previous history of velocities on the current velocity. A large inertia weight factor facilitates global exploration (i.e., searching of new area) while small weight factor facilitates local exploration. Therefore, it is better to choose large weight factor for initial iterations and gradually reduce weight factor in successive iterations. This can be achieved by using Equation 4.5.

$$W = W_{max} - (W_{max} - W_{min}) * \frac{Iter}{Iter_{max}} \quad (4.5)$$

where $max$ and $W_{min}$ are initial and final weight respectively, $Iter$ is current iteration number and $Iter_{max}$ is maximum iteration number.

Acceleration constant $C_1$ called cognitive parameter pulls each particle towards local best position whereas constant $C_2$ called social parameter pulls the particle towards global best position[29]. The particle position is modified by Equation 4.4. The process is repeated until stopping criterion is reached.

The number of threshold levels is the dimension of the problem. For example, if there are "m" threshold levels, the i'th particle is represented as follows:

$$X_i = (X_{i,1}, X_{i,2}, ...., X_{i,m}) \tag{4.6}$$

Its implementation consists of the following steps:

- Initialization of the swarm: For a population size $p$, the particles are randomly generated between the minimum and the maximum limits of the threshold values.

- Evaluation of the objective function: The objective function values of the particles are evaluated using the objective functions.

- Initialization of *pbest* and *gbest*: The objective values obtained above for the initial particles of the swarm are set as the initial *pbest* values of the particles. The best value among all the *pbest* values is identified as *gbest*.

- Evaluation of velocity: The new velocity for each particle is computed using the Equation.

- Update the swarm: The particle position is updated using Equation 4.3. The values of the objective function are calculated for the updated positions of the particles. If the new value is better than the previous *pbest*, the new value is set to *pbest*. Similarly, *gbest* value is also updated as the best *pbest*.

- Stopping criteria: If the stopping criteria is met, the positions of particles represented by *gbest* are the optimal threshold values. Otherwise, the procedure is repeated from step 4.

There are many advantages of PSO. They include:

1. PSO is easy to implement and only a few parameters have to be adjusted.
2. Unlike the GA, PSO has no evolution operators such as crossover and mutation.
3. In GA, chromosomes share information so that the whole population moves like one group, but in PSO, only global best particle (*gbest*) gives out information to the others. It is more robust than GA.
4. PSO can be more efficient than GA; that is, PSO often finds the solution with fewer objective function evaluations than that required by GA [19].
5. Unlike GA and other heuristic algorithms, PSO has the flexibility to control the balance between global and local exploration of the search space.

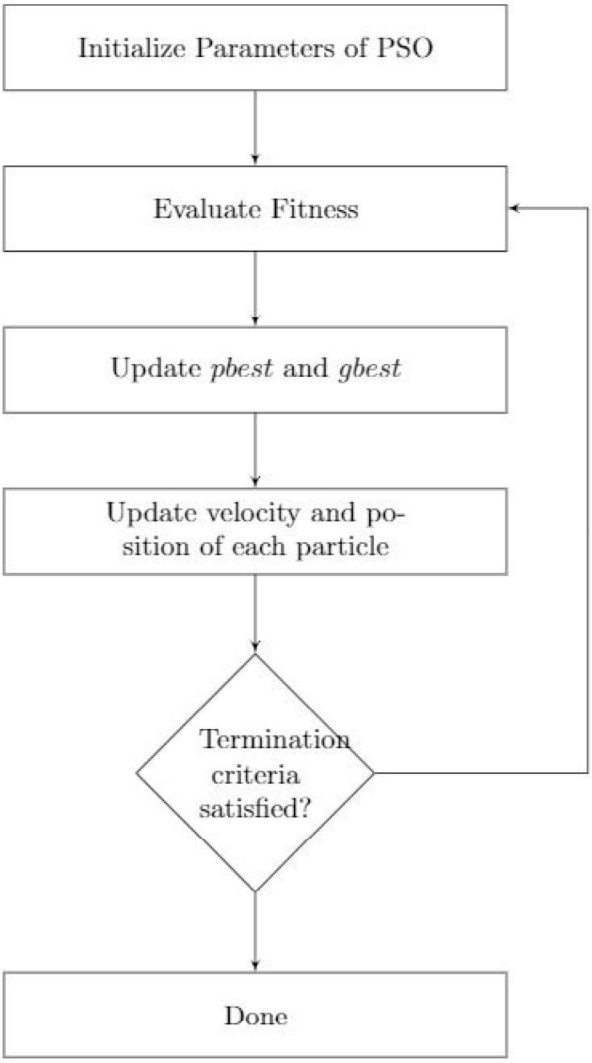


**Figure 4.3.** PSO process flow

# CHAPTER 5

## RESEARCH OVERVIEW

The current research on oil spill detection focuses on sensors technologies and the image processing techniques of the data produced by these sensors. Each sensor technology is based on different image processing techniques, which are in turn dependent on the data produced by it. Almost every oil spill detection process based on Synthetic Aperture Radar (SAR) sensor technology, follows the same processing sequence. However, each research study has its own method of processing and each aim at enhancing the process of detecting the oil spill.

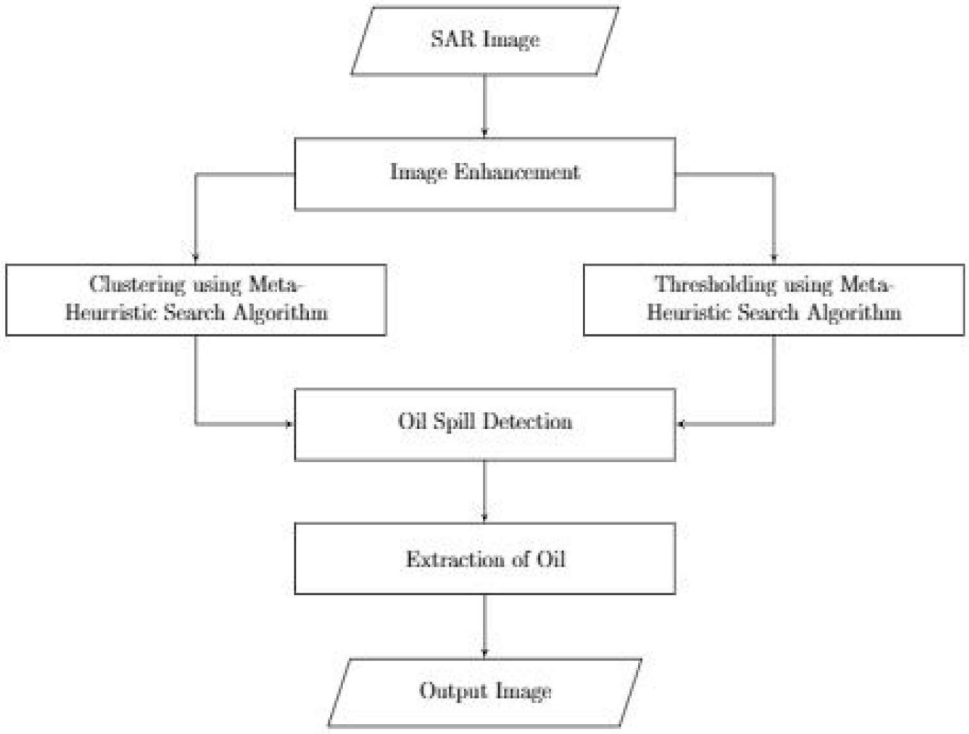


**Figure 5.1.** System design

To achieve the criteria required for high efficiency.A framework to detect the oil spill in SAR images is proposed. Our framework as shown in Figure 5.1, shows each stage of our method, which is summarized in the following steps:

1. SAR image enhancement, which includes:
   (a) Contrast Stretching.
   (b) Noise removal based filter.
2. Image segmentation
   (a) Clustering
   (b) Thresholding
3. After segmentation oil will be classified as an oil spill.
4. Finally, each oil spill will be marked.

## 5.1 SAR Image Database

Satellite instruments are well adapted to monitor and therefore to detect oil pollution since they regularly produce images of the sea surface including the remote areas. Several kinds of measurements have been tested: optical, infrared, radars with different frequencies. Here the main attention will be given to consideration of oil spills on Synthetic Aperture Radar (SAR) images. SAR seems to be one of the most suitable instruments for the detection of slicks, since slicks damp strongly short waves measured by SAR and oil spills appear as a dark patch on the SAR image. SAR observations do not depend on weather (clouds) and sunshine, which allows showing illegal discharges that most frequently appear during the night. The images that are used in this research are taken by satellites RADARSAT-1 and JERS-1 which has the image scale of 2km by 2km and 2.5km by 3km respectively.

## 5.2 Image Enhancement

The study requires pre-processing of images, which can be applied before segmentation stage. The effect of noise causes grainy appearance in the radar image which disrupts visual interpretation. In order to solve this problem, we propose the following enhancement techniques:

- Wiener Filter
- Vector Median Filter

These enhancement techniques enhance the intensity and remove the noise from SAR images. Figure 5.2 shows the proposed image enhancement stage.

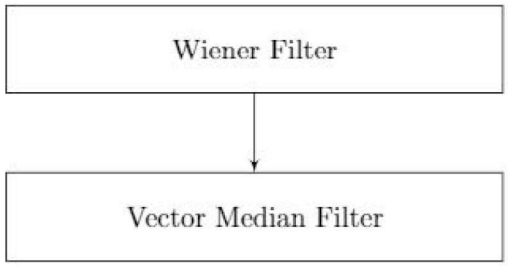


**Figure 5.2.** Image Enhancement stage

### 5.2.1 Wiener Filter

The inverse filtering is a restoration technique for deconvolution, i.e. when the image is blurred by a known low pass filter, it is possible to recover the image by inverse filtering or generalized inverse filtering. However, inverse filtering is very sensitive to additive noise. The approach of reducing one degradation at a time allows us to develop a restoration algorithm for each type of degradation and simply combine them.

The wiener filtering executes an optimal trade-off between inverse filtering and noise smoothing. It removes the additive noise and inverts the blurring simultaneously [16].

The Wiener filtering is optimal in terms of the mean square error. In other words, it minimizes the overall mean square error in the process of inverse filtering and noise smoothing. The Wiener filtering is a linear estimation of the original image. The approach is based on a stochastic framework.

Wiener filter filters the given image using pixel-wise adaptive Wiener filtering, using neighborhoods of size M-by-N to estimate the local image mean and standard deviation. If you omit [M N] argument, M and N default to 3. The additive noise (Gaussian white noise) power is assumed to be noise but the images that are given as input do not have specific gaussian noise. so the speckle noise in the SAR images are considered as noise and the Wiener filter calculation is modified in a way that suits for the speckle noise. The modified wiener filter is represented using Equation 5.1.

$$\widehat{F}(u,v) = \frac{|H(u,v)|^2}{H(u,v)|H(u,v)|^2 + |N(u,v)|^2/|F(u,v)|^2} G(u,v), \tag{5.1}$$

where $H(u,v)$ is the degradation function, $G(u,v)$ is the Fourier transform of the degraded image, $|N(u,v)|^2$ is the power spectrum of noise, $|F(u,v)|^2$ is the power spectrum of the undegraded image. The Wiener filter performs deconvolution in the sense of minimizing a least squares error i.e.:

$$e^2 = E(f - \widehat{f})^2 \tag{5.2}$$

where E is the mean value, f is the undegraded image which is usually not known. In the case of omitting the noise the Wiener filter changes to a simple inverse filter.

### 5.2.2 Vector Median Filter

Vector median filter performs median filtering of the matrix in two dimensions. Each output pixel contains the median value in the M-by-N neighborhood around the corresponding pixel in the input image [35]. This median filter pads the image with zeros on the edges, so the median values for the points within [M N]/2 of the edges may appear distorted.

## 5.3 Segmentation based Clustering

Clustering refers to the process of grouping samples (or data) so that the samples are similar within each group. The groups are called clusters. Clustering algorithms are used in many applications, such as pattern recognition, image analysis, data mining and machine learning.

A widely used partitional clustering algorithm is the Kmeans clustering algorithm. K-means clustering groups data vectors into a predefined number of clusters, based on the Euclidean distance as similarity measure. Data vectors within a cluster have small Euclidean distance from one another, and are associated with the centroid vector, which represents the mean of the data vectors that belong to the cluster. The K-means clustering has the following two main advantages. It is easy to implement and the time complexity is only $O(n)$ (where n is the number of data points), which makes it suitable for large data sets. However, its performance depends on initial conditions, which may cause the algorithm to converge to suboptimal solutions.

In order to overcome the above mentioned limitation, in this research, an efficient clustering technique, that utilizes an effective integration of Meta-heuristic search algorithms are developed.

| $X_1$ | $Y_1$ | $X_2$ | $Y_2$ | $X_3$ | $Y_3$ |
|---|---|---|---|---|---|

**Figure 5.3.** Problem representation

### 5.3.1 Problem Representation

To compute the fitness, suppose V=$v_1, v_2, v_3$ be a chromosome that each of its members is the center of each cluster as shown in Figure 5.3.

### 5.3.2 Fitness Function For Clustering Methods

The qualification of each member of the community is determined by using fitness function after creating initial community. By using a fitness function, a number is assigned to each chromosome which is the value of that chromosome. This number is used as a merit determining the presence of this chromosome for the next generation.

To compute the fitness, suppose V=$v_1, v_2, v_3.....v_k$ be a chromosome that each of its members is the center of each cluster. Thus, a fitness function is computed as given in Equation 5.3.

Here $|v_i - v_j|$ is the distance between the cluster centers of i and j , $\sum_{t=1}^{n_1} |v_i - x_l|$ and $\sum_{p=1}^{n_2} |v_j - x_h|$ are the sum of differences between i and j cluster members and the cluster centers, $n_1$ and $n_2$ are the number of i and j cluster members. To obtain the optimal clustering, the purpose is to increase the fitness required, which is equivalent to clustering with minimum distribution into clustering and minimum separation between cluster centers. Mathematically, is defined for k clusters $c_1, c_2, c_3....c_k$ as shown in Equation 5.3.

$$F(c_1, c_2, c_3....c_k) = \sum_{i=1}^{k} \sum_{x_j \in c_i} ||x_j - z_i||^2 \tag{5.3}$$

Here $z_i$ represents the center of cluster $c_i$ represents a data point $x_j$ belonging to cluster $c_i$. The goal is to search for the appropriate cluster centers $z_1, z_2.....z_k$ such that the clustering criterion F is minimized.

### 5.3.3 Segmentation based on clustering using GA

Before segmentation using GA the main factors that need to be considered [18] are explained below.

- Chromosome representation: In the proposed GA a chromosome indicates the cluster centers. Suppose that the oil spill image is two dimensions, $l_i$ as the i'th chromosome length which is $2 \times k_i$, and $k_i$ as the number of clusters.

- Generating Initial Population: For each $I$ chromosome, the initial population is produced randomly from the surrounding borders of the image. After generating initial population, the qualification of each chromosome is obtained from the fitness function given in equation 5.3. After finding the chromosome with optimal cluster centers, the process of clustering must be applied to the Oil spill images using the cluster centers obtained.

### 5.3.4 Segmentation based on clustering using SA

Likc thc K-mcans algorithm, thc anncaling-cvolution proccss trics to minimizc thc intracluster spread (ICS) as shown in Equation 5.3.

In the clustering algorithm, a pool, P, of probable solutions or configurations are maintained [27]. Each member of the pool (also called population) is represented as a string of vectors, each identifying a cluster center. For each member of the pool, the data points are initially assigned to clusters, known a priori, randomly, and the

cluster centers are computed. Thus we get a number of clustering solutions equal to the population size.

For each configuration (solution string), we compute its energy value as the corresponding sum of distances between cluster centers and cluster points. The solutions which are potentially better, having lower energy values, are selected with higher probability and used in the mutation phase. At each temperature, K, a new pool is generated from the older one by the processes of selection and mutation.

### 5.3.5 Segmentation based on clustering using PSO

Same as the K-means clustering algorithm, PSO tries to minimize the intracluster spread as shown in Equation 5.3. Every particle is randomly assigned to specific cluster centers. During each iteration, the velocity of the particles gets changed using the Equation 4.3.

The fitness function given in Equation 5.3 is the sum of distances. The fitness function is thus a multi-objective problem. Approaches to solving multi-objective problems have been developed mostly for evolutionary computation approaches. Since the focus of this thesis is to work on the applicability of Meta-heuristic search algorithms to image clustering, and not on multi-objective optimization, here we use a simple approach to cope with multiple objectives. Different priorities are assigned to the sub-objectives through appropriate initialization of the values of $w1$ and $w2$. Experimental results have shown that the PSO image classier to improve the performance of the K-means algorithm. Here we propose a different fitness function, i.e equation 5.3.

| $X_1$ | $Y_1$ | $X_2$ | $Y_2$ |
|---|---|---|---|

**Figure 5.4.** Problem representation

## 5.4 Segmentation based Thresholding

Thresholding is the easiest method for segmentation as it works by taking a threshold value so that pixels whose intensity value is higher than a threshold are labeled as the first class while the rest correspond to a second-class label. When the image is segmented into two classes, the task is called bi-level thresholding (BT) and requires only one threshold value. On the other hand, when pixels are separated into more than two classes, the task is named as MT and demands more than one threshold value. In this work basic thresholding technique is improved using Meta-heuristic search algorithms.

### 5.4.1 Problem Representation

To compute the fitness, suppose T=$t_1, t_2$ will be a chromosome and each of its members is the threshold value as shown in Figure 5.4.

### 5.4.2 Fitness Function For Thresholding Methods

The qualification of each member of the community is determined using fitness function after creating initial community. By using this fitness function, a number is assigned to each chromosome which is the value of that chromosome. This number is used as a merit determining the presence of this chromosome for the next generation or iteration.

The Otsu based thresholding algorithm can be described as follows:

If an image can be divided into two classes, $C_0$ and $C_1$, by a threshold at a level

$t$, class $C_0$ contains the gray levels from 0 to $t-1$ and class $C_1$ consists of the other gray levels with $t$ to $L-1$ [37]. Then, the gray level probabilities and distributions for the two classes are as follows:

$$C_0 : \frac{P_0}{w_0} \ldots \frac{P_{t-1}}{w_0} \quad C_1 : \frac{P_t}{w_1} \ldots \frac{P_{L-1}}{w_1} \tag{5.4}$$

where $w_0 = \sum_{t=1}^{t-1} P_t$ and $w_1 = \sum_{i=t}^{L-1} P_t$

Mean levels $\mu_0$ and $\mu_1$ for classes $C_0$ and $C_1$ are as follows:

$$\mu_0 = \sum_{i=0}^{t-1} \frac{iP_t}{w_0}, \quad \mu_1 = \sum_{i=t}^{L-1} \frac{iP_t}{w_1} \tag{5.5}$$

Let $\mu_T$ be the mean intensity for the whole image, it is easy to show that

$$w_0\mu_o + w_1\mu_1 = \mu_T \quad and \quad w_0 + w_1 = 1 \tag{5.6}$$

Using discriminant analysis, Otsu between-class variance thresholded image can be defined as follows:

$$f(t) = \sigma_0 + \sigma_1 \tag{5.7}$$

where:

$$\begin{aligned} \sigma_0 &= w_0(\mu_0 - \mu_T)^2 \\ \sigma_1 &= w_1(\mu_1 - \mu_T)^2 \end{aligned} \tag{5.8}$$

Thus the fitness function to segment the image has been developed in this work, This fitness function is used to calculate the multi level threshold in an image:

$$\sigma = w_0(\mu_{01} - \mu_{T1})^2 + w_{11}(\mu_{11} - \mu_{T1})^2 + w_2(\mu_{02} - \mu_{T2})^2 + w_3(\mu_{11} - \mu_{T2})^2 \tag{5.9}$$

From the fitness function we developed, Otsu selects an optimal threshold $t_1$ and $t_2$ that minimizes the sum of intraclass variance. From Equation 5.9 we can see the improved Otsu single level threshold to bi-level threshold. Intraclass variance is calculated for two threshold values and the lease sum is chosen as the best intraclass variance and the threshold values will be used to segment the image.

### 5.4.3 Segmentation based on thresholding using GA

In the following, we provide the steps followed to provide our results.

- Step 1: On using GA, it is necessary to encode the value of the solution space to produce the chromosome element. Since the grayscale image contains 256 gray levels, it corresponds to one byte, so one byte is used as a chromosome. The decoding process of a chromosome is exactly the inverse of the encoding process, which is the decimal number of a byte.

- Step 2: Initializing population: We produce 100 populations in the optimal threshold range $[T_1, T_2]$. The population is obtained by average distribution.

- Step 3: Calculate the fitness shown in Equation 5.7. In this work, we take the maximum of variance $\sigma^2(k)$ as the goal, so we use $\sigma^2(k)$ as individual fitness.

- Step 4: Select and inter-cross population We use traditional method in GA to select and inter-cross population. In selection, we use the probability proportional to fitness to determine the number of individuals copied to the next-generation population.

- Step 5: Mutation: Some genetic variation may result in the loss of some effective genes. In order to recover these effective genes and maintain the diversity

of the population, when the mutation rate is increased when the individual is in a local optimum and reduced when the rate of variation is for a high fitness individual.

- Step 6: Ending condition The algorithm terminates when the evolutionary algorithm computes all the thresholds in the optimal threshold range $[T_1, T_2]$, or if the optimal individuals within the population have not changed in 5 generations of evolution. Otherwise, go to step 3.

### 5.4.4 Segmentation based on thresholding using SA

Like the Otsu segmentation algorithm, the annealing-evolution process tries to minimize the intraclass variance (ICV). Mathematically, it is defined for k thresholds $t_1, t_2, t_3....t_k$ as shown in Equation 5.7.

In this algorithm, a pool, P, of probable solutions or configurations are maintained. Each member of the pool (also called population) is represented as a string of vectors, each identifying threshold values. For each member of the pool, the data points are initially assigned to threshold values, known a priori, randomly, and the threshold values are computed. Thus we get a number of segment solutions equal to the population size. For each configuration (solution string), we compute its energy value as the corresponding ICS. The fitness value of the string is correspondingly calculated as $\frac{1}{ICS}$. The solutions which are potentially better, having lower energy values, are selected with higher probability and used in the mutation phase. At each temperature, K, a new pool is generated from the older one by the processes of selection and mutation.

### 5.4.5 Segmentation based on thresholding using PSO

The multilevel image thresholding problems using the PSO algorithm. The number of threshold levels is the dimension of the problem. For example, if there are m threshold levels, the i'th particle is represented as follows: $X_i = (X_{i1}, X_{i2}, ., X_{im})$

It's implementation consists of the following steps:

- Step 1: Initialization of the swarm: For a population size p, the particles are randomly generated between the minimum and the maximum limits of the threshold values.

- Step 2: Evaluation of the objective function: The objective function values of the particles are evaluated using the objective function using the equation 5.7.

- Step 3: Initialization of *pbest* and *gbest*. The objective values obtained above for the initial particles of the swarm are set as the initial *pbest* values of the particles. The best value among all the *pbest* values is identified as *gbest*.

- Step 4: Evaluation of velocity: The new velocity for each particle is computed using Equation 4.3.

- Step 5: Update the swarm: The particle position is updated using Equation 4.4. The values of the objective function are calculated for the updated positions of the particles. If the new value is better than the previous *pbest*, the new value is set to *pbest*. Similarly, *gbest* value is also updated as the best *pbest*.

- Step 6: Stopping criteria: If the stopping criteria are met, the positions of particles represented by *gbest* are the optimal threshold values. Otherwise, the procedure is repeated from step 4.

## 5.5 Extraction of Oil

After segmentation stage, we need to extract oil from the segmented image, which guides us to differentiate oil and water easily. Subsequently, we calculate the area of the segmented oil. Area of the segmented oil represents the number of pixels in this region. We can compute the number of pixels for each segmented object that is oil and mixture in this case.

# CHAPTER 6

# TESTING AND EVALUATION

This chapter presents the testing results of our proposed oil spill detection method. The entire procedures are completely described. All our algorithms were implemented in MATLAB. The SAR images used here all of the grayscale types. The proposed method was presented in Figure 5.1.

We will discuss and present The results of each of the following stages are presented in detail in the next sections.

- Image Enhancement
    1. Wiener Filter
    2. Vector Median Filter
- Segmentation
    1. Clustering
    2. Thresholding
- Oil Area Extraction

## 6.1 Image Enhancement

In this section, we present the first stage of our proposed methodology for the enhancement, which is the pre-processing stage for segmentation. This stage consists of two sub stages, they are (a) Wiener filter, (b) Vector median filter.

### 6.1.1 Wiener Filter

Wiener filter was applied to the SAR image to improve the image quality. In Figure 6.1, we show the original SAR image and the SAR image after Wiener filter. We noticed that SAR image after Wiener filter tends to remove the Gaussian white noise. We conclude that the Wiener filter method has better characteristics than the original image. The gray scale levels are extended to wide range than the original image. The histograms of the original and Wiener filter images are shown in the Figure 6.2

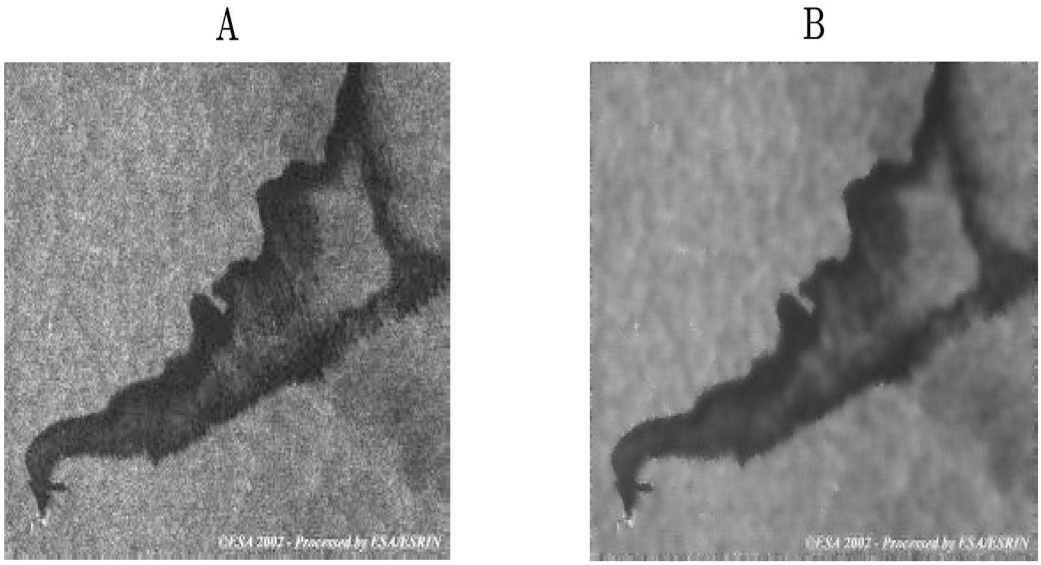


**Figure 6.1.** (A): Original image given as input (B): The resultant image obtained after applying Wiener filter

### 6.1.2 Vector Median Filter

Vector median filter was applied to the output image obtained from the Wiener filter. The reason is, Vector Median Filter can smooth the image.This will help differentiate threshold values that lie on the edges of different segments in the image, which will

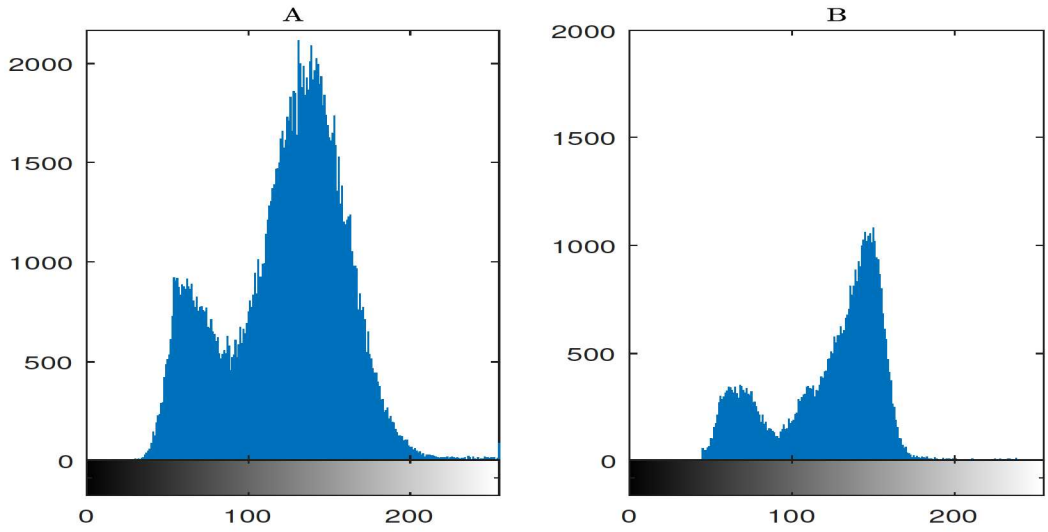


**Figure 6.2.** (A): Histogram of original image (B): Histogram of image after applying Wiener filter

minimize the classification in the threshold values. The output image obtained from the vector median filter is shown in Figure 6.3 and the histograms of the images are shown in Figure 6.4.

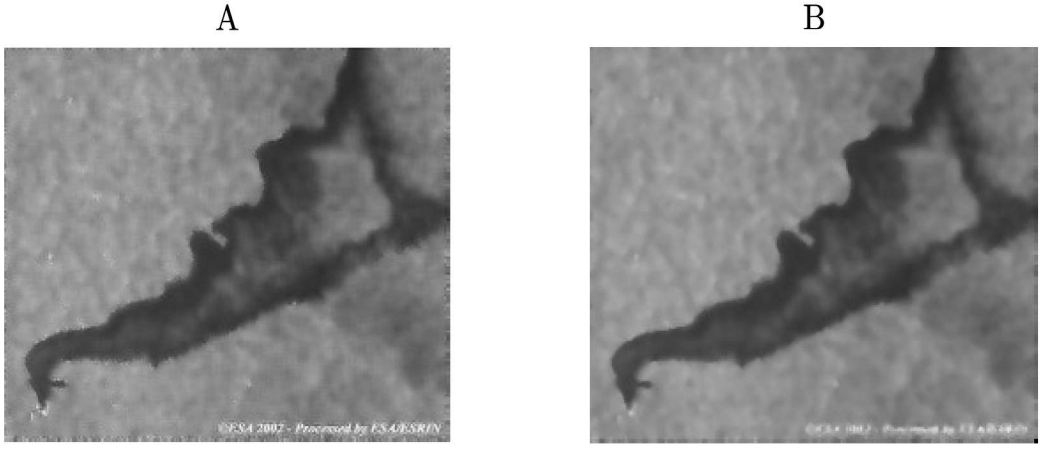


**Figure 6.3.** (A): Original image given as input (B): The resultant image obtained after applying Vector median filter

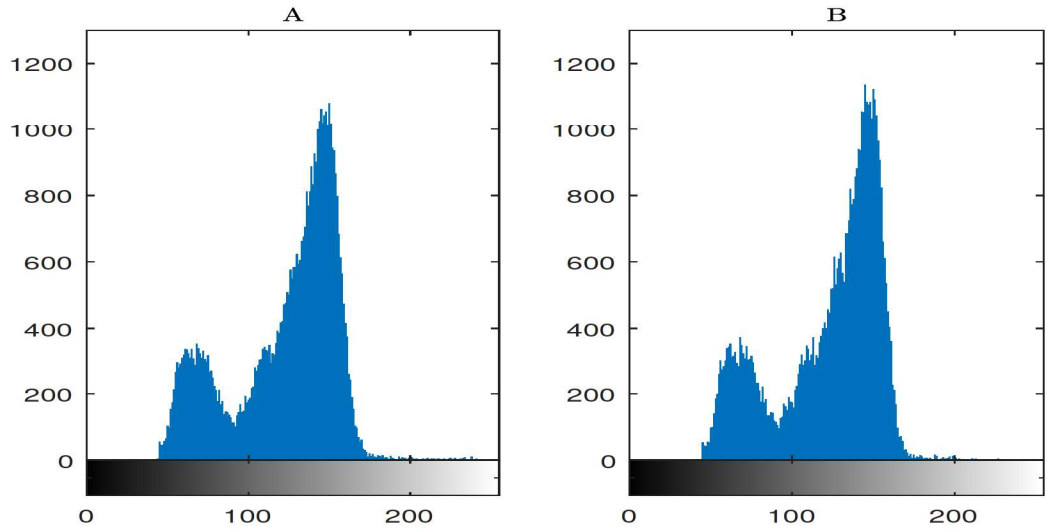


**Figure 6.4.** (A)Histogram of input image (B): Histogram of image after applying vector median filter of the images shown in the figure 6.3

## 6.2 Clustering based segmentation results

Different clustering algorithms show different results, and evaluating those results is very important. Thus, cluster validity has become a very important challenge. In this work, the proposed model is compared with a K-means algorithm, FCM and different clustering techniques using Meta-heuristic search algorithms.

The results obtained from the framework using K-means, FCM, GA, SA, PSO are analyzed. In each case, the input image, preprocessed image, segmented image and the oil extracted images are displayed.

The images are preprocessed and then segmented using K-means algorithm and the results obtained are shown in the Figure 6.7 and the intra cluster spread are tabulated in the Table 6.3.

FCM is also implemented on the same images and the results are displayed in Figure 6.8. Figure 6.9 shows the result that is obtained using GA. The segmentation is implemented by finding the optimal cluster centers using GA and then these centers

Table 6.1. Tuning Parameters for GA implementation

| Parameter | Value |
|---|---|
| Population | 60 |
| Generations | 100 |
| Chromosome length | 3 |
| Crossover rate | 0.8 |
| Selection rate | 0.4 |

are used to segment the image by partitioning the pixels of the image to its closest cluster. Here we propose segmenting an image into three clusters, so three optimal cluster centers are obtained using GA. The obtained centers are given in Table 6.4. The three clusters in the segmented image are oil, water, and the mixture of oil and water. The oil and the mixture are combined into a single cluster and a binary image is formed and displayed, which only displays the oil and water. The set of parameters which consistently lead to good results are shown in Table 6.1 and the convergence curves when different population sizes are used are shown in Figure 6.5.

The same process is repeated again but here the Meta-heuristic search algorithms used is SA. We use SA to find the optimal cluster centers which are shown in Table 6.4 and the resultant images that are obtained from this method are shown in Figure 6.10. PSO is also used to find the optimal cluster and the results obtained by using PSO are shown in Figure 6.11 and the parameters with which the PSO algorithm works well are shown in Table 6.2 and the convergence curves when different swarm size is used is shown in Figure 6.6.

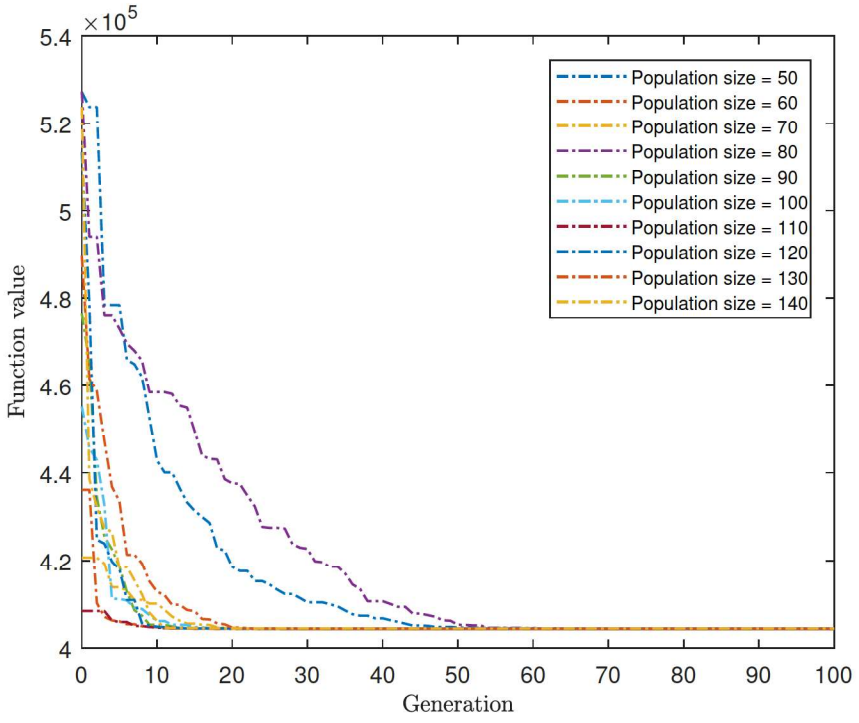


**Figure 6.5.** Convergence curves with different population size

### 6.2.1 Best so-far Curves

The convergence curves for the proposed Meta-heuristic search algorithms are shown below and the fitness function for which the curves are attained is given by Equation 6.1. The three methods are compared using the sum of the distance between cluster centers and the cluster points, The more the distance the more the difference between the clusters. Table 6.3 shows the distance obtained for each method

$$d = \sum_{i=1}^{k} \sum_{x_j \in c_i} ||x_j - z_i||^2 \tag{6.1}$$

The convergence curve that is obtained when the framework is applied using GA is shown in Figure 6.12. In convergence curve 6.13, we can see the best, mean and worst fitness curves that are obtained by using a Meta-heuristic search algorithm

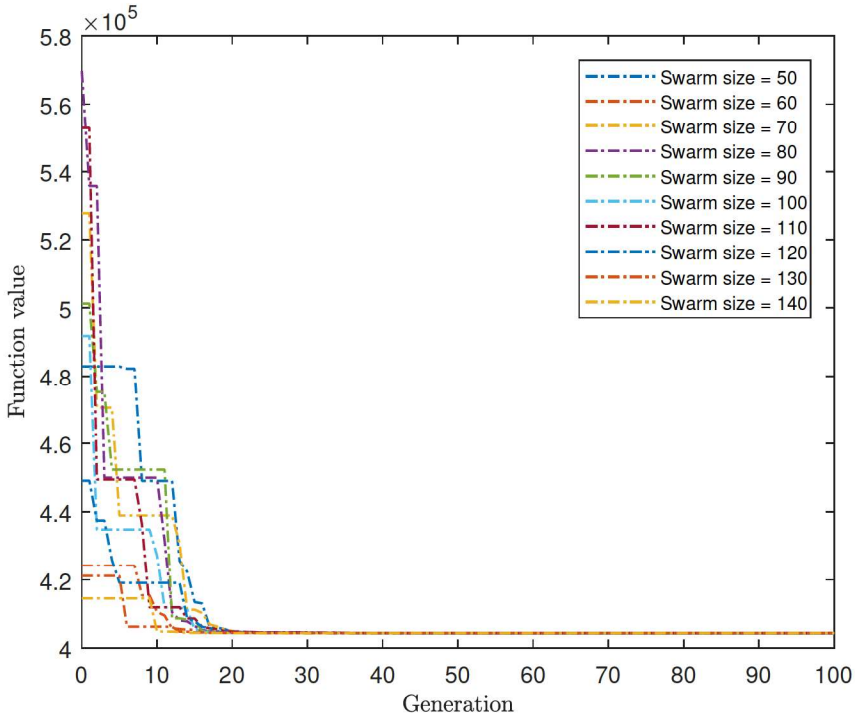


**Figure 6.6.** Convergence curves with different Swarm size

for 10 iterations. Figure 6.14 and Figure 6.16 show the convergence curves that are obtained when the framework is implemented using SA and PSO over 10 iterations and the best, mean and worst curves are shown in Figures 6.15 and 6.17 .

The methods are also compared using the time taken to process the image. Table 6.5 shows the amount of oil that is extracted from each image calculated in the form of pixels.

Even though the time taken for the K-means algorithm is less compared to clustering using PSO, the intracluster spread obtained for a cluster using PSO is significantly less compared to result from K-means. Table 6.3 shows the results that are obtained from the above methods. We can deduce that Clustering using PSO provides the best cluster centers compared to other methods. This conclusion is based on the evaluated distance given in Table 6.3.

Table 6.2. Tuning Parameters for PSO implementation

| Parameter | Value |
|---|---|
| Swarm size | 50 |
| Iterations | 100 |
| Individual Weight | 0.9 |
| Social Weight | 0.4 |
| Inertial Factor | 1.2 |

| Algorithm | Fitness value | Improvement |
|---|---|---|
| K-means | 407947 | - |
| FCM | 406655 | 1292 |
| SA | 404420.0073 | 3526.993 |
| GA | 404371.0422 | 3575.688 |
| PSO | 404360.0001 | 3587.999 |

Table 6.3. Fitness values(i.e sum of distances) and improvement based on Sum of cluster distances compared to K-means

Table 6.4. Computed Cluster Centers for various methods

| Algorithm | Cluster Centers |
|---|---|
| K-means | [69.0043, 117.4087, 147.4352¿ |
| FCM | [68.1199, 118.78, 148.294] |
| GA | [68.99907, 121.0126, 147.99987] |
| SA | [69, 120, 147] |
| PSO | [69, 121, 147.9999] |

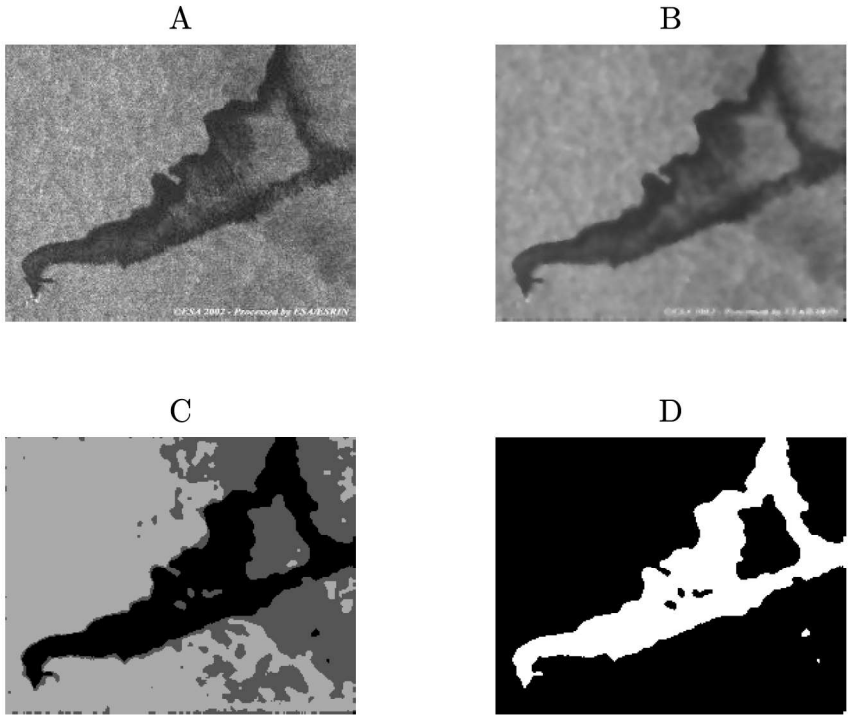


**Figure 6.7.** Clustering using K-means (A): Original image (B): Pre-processed image (C): Segmented image (D): Oil extracted image

## 6.3 Thresholding Results

The results obtained from the framework using GA, SA, PSO are shown in Figures 6.18,6.19 and 6.20 and in each of the figure there is an input image, preprocessed image, segmented image and the processed image in which the oil is extracted.

Figure 6.18 shows the results obtained using GA. In this image, we can see the resultant image obtained after the preprocessing stage and the segmented image. The segmentation is performed by finding the optimal threshold values that give less intraclass variance using GA and then these threshold values are used to segment the image. The image is segmented into three clusters, so two optimal threshold values are obtained using GA. The obtained threshold values are given in Table 6.7. The three clusters in the segmented image are oil, water, and the mixture of oil and

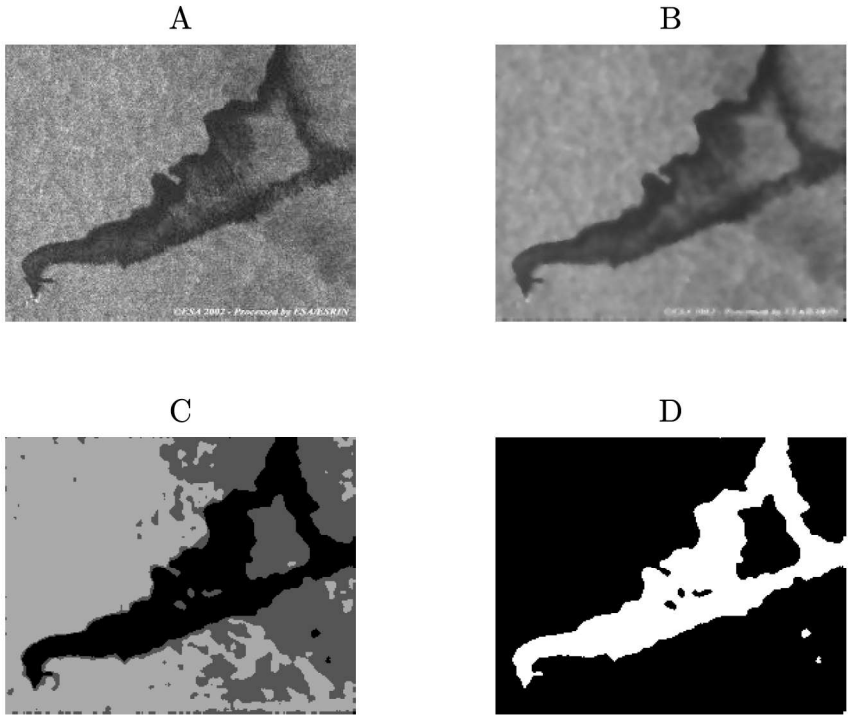


**Figure 6.8.** Clustering using FCM (A): Original image (B): Pre-processed image (C): Segmented image (D): Oil extracted image

water. The water and a mixture are combined into a single cluster and a binary image is formed and displayed, which only displays the oil and water. The same process is repeated again with the use of SA. The optimal threshold values with less intraclass variance are tabulated in Table 6.7 and the resultant images obtained from this method are shown in Figure 6.19. PSO is also used to find the optimal cluster and the results obtained by using PSO are shown in Figure 6.20.

### 6.3.1 Best so-far Curves

The convergence curves the for the Meta-heuristic search algorithms are shown in Figures 6.22, 6.24 and 6.26 and the fitness function for which the curves are attained is given by Equation 6.2

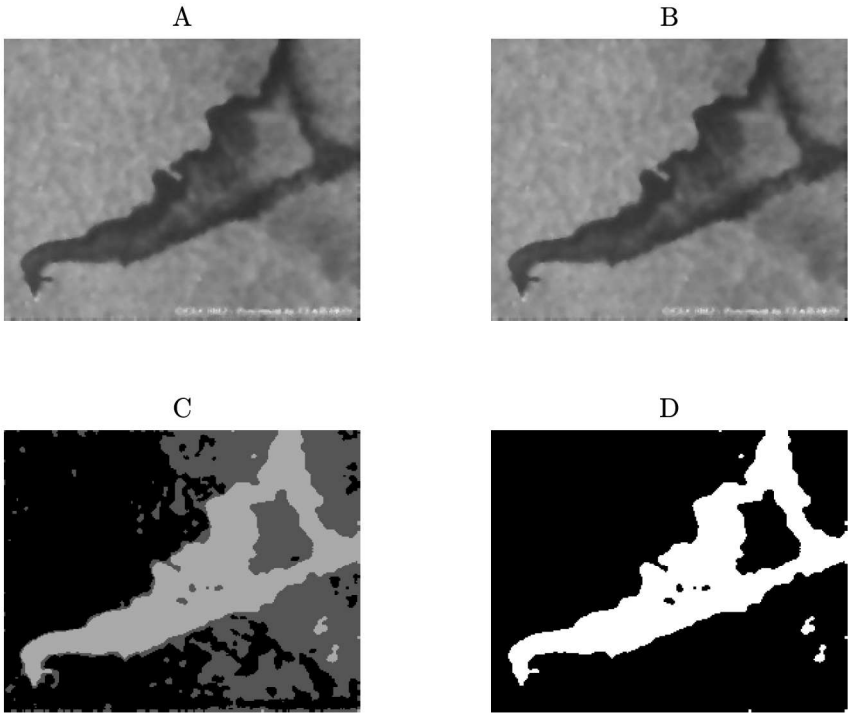


**Figure 6.9.** Clustering using GA (A): Original image (B): Pre-processed image (C): Segmented image (D): Oil extracted image

$$f(t) = \sigma_0 + \sigma_1 \tag{6.2}$$

where $\sigma_0 = w_0(\mu_0 - \mu_T)^2$ and $\sigma_1 = w_1(\mu_1 - \mu_T)^2$

The convergence curve that is obtained when the framework is performed using GA is shown in Figure 6.21. In convergence curve 6.22, we can see the best, mean and worst fitness curves that is obtained by using specific Meta-heuristic search algorithms when executed 10 times. Figure 6.23 and Figure 6.25 shows the convergence curves that are obtained when the framework is performed using SA and PSO for 10 runs and the best, mean and worst curves are shown in the Figures 6.24 and 6.26.

The three methods are compared using the intraclass variance, the less the variance more the difference between the segmented parts of the image. Table 6.6 shows

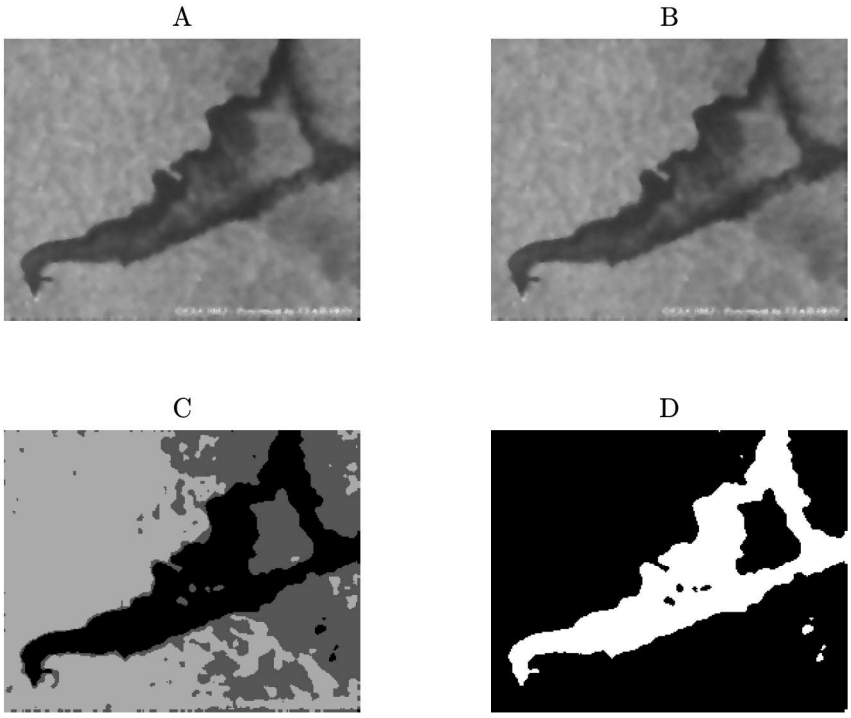


**Figure 6.10.** Clustering using SA (A): Original image (B): Pre-processed image (C): Segmented image (D): Oil extracted image

the intraclass variance obtained using different Meta-heuristic search algorithms. The methods are also compared using the time taken to process the image. Table 6.8 shows the amount of oil that is extracted from each image which is calculated in the form of pixels.

The time taken for thresholding using PSO is almost 60% more than Otsu method but the intraclass variance is almost 35% less that Otsu method. The intraclass variance obtained using SA and GA are also less compared to Otsu method but PSO outperforms all other methods. From the results shown in Tables 6.6 we can deduce that thresholding using PSO gives good results compared to the other methods that are used.

Table 6.5. Amount of Oil extracted from an image measured in terms of square kilometers

| Meta Heuristic Algorithm Type | Total Size (Sq Km) | Extracted Oil (Sq Km) |
|---|---|---|
| K-means | 2 | 0.5104 |
| FCM | 2 | 0.5391 |
| Genetic Algorithm | 2 | 0.4324 |
| Simulated Annealing | 2 | 0.5427 |
| Particle Swarm Optimization | 2 | 0.4391 |

Table 6.6. Intra class variance and the improvement compared to Otsu

| Algorithm Type | Intra class variance | % Improvement |
|---|---|---|
| Otsu | 63240.3 | - |
| GA | 57900.7 | 5339.3 |
| SA | 57774.3 | 5466 |
| PSO | 40436.0001 | 22804.299 |

Table 6.7. Obtained threshold values for Thresholding method

| Algorithm Type | Threshold values |
|---|---|
| Otsu | [104 , 148] |
| GA | [104 , 149] |
| SA | [103 , 147] |
| PSO | [104 , 147] |

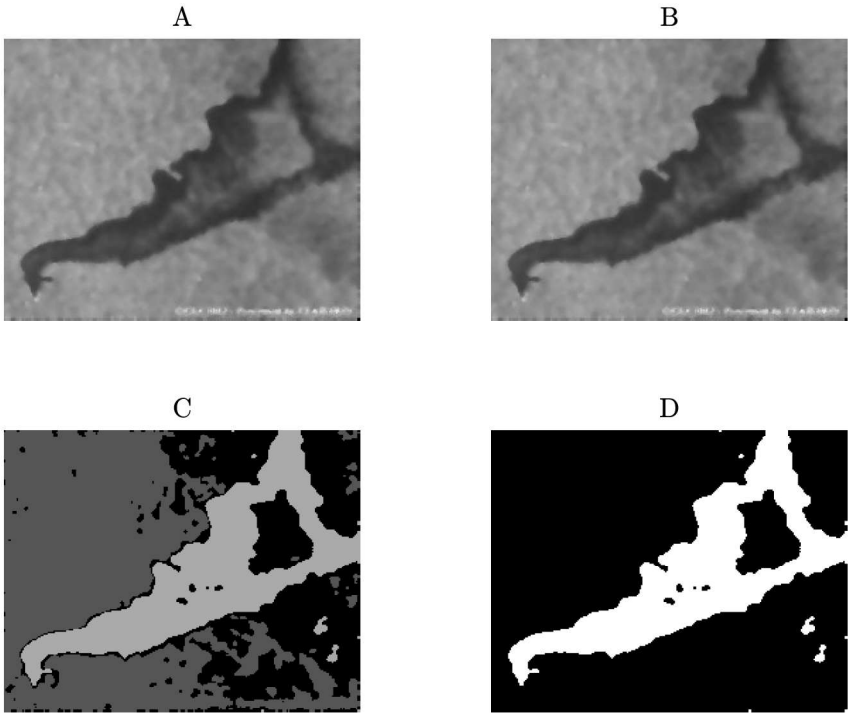


**Figure 6.11.** Clustering using PSO (A): Original image (B): Pre-processed image (C): Segmented image (D): Oil extracted image

## 6.4 Oil extraction

In this stage, a binary image is obtained by selecting a threshold value to convert the segmented image to binary image where the water and mixture are combined and the oil is separated. The extracted oil is calculated in the form of pixels and is displayed in the form of a table for both segmentation frameworks using different Meta-heuristic search algorithms.

Some of the sample database images for which the extraction performed is shown in Figures 6.27, 6.28, 6.29, 6.30 and 6.31

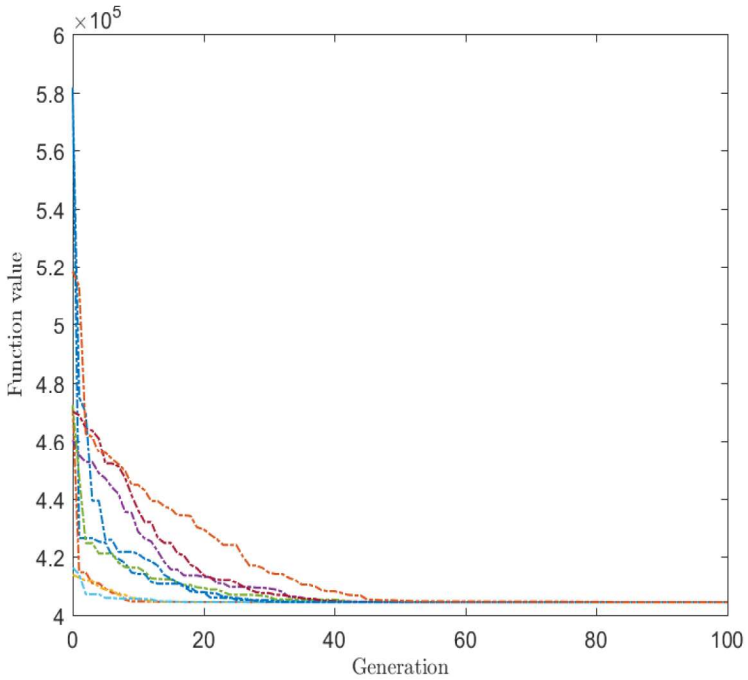


**Figure 6.12.** Convergence curves for Clustering using GA for 10 runs

Table 6.8. Amount of Oil extracted from an image measure in terms of square kilometer

| Meta Heuristic Algorithm Type | Total Size (Sq Km) | Extracted Oil (Sq Km) |
|---|---|---|
| Otsu | 2 | 0.4909 |
| GA | 2 | 0.4967 |
| SA | 2 | 0.5392 |
| PSO | 2 | 0.4797 |

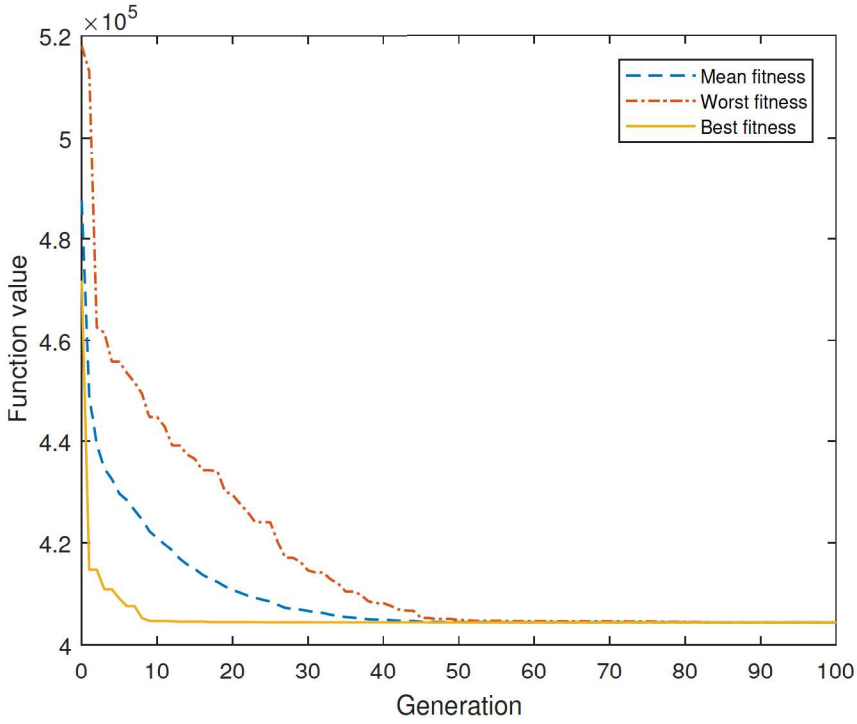


**Figure 6.13.** Best so-far curve for Clustering using GA

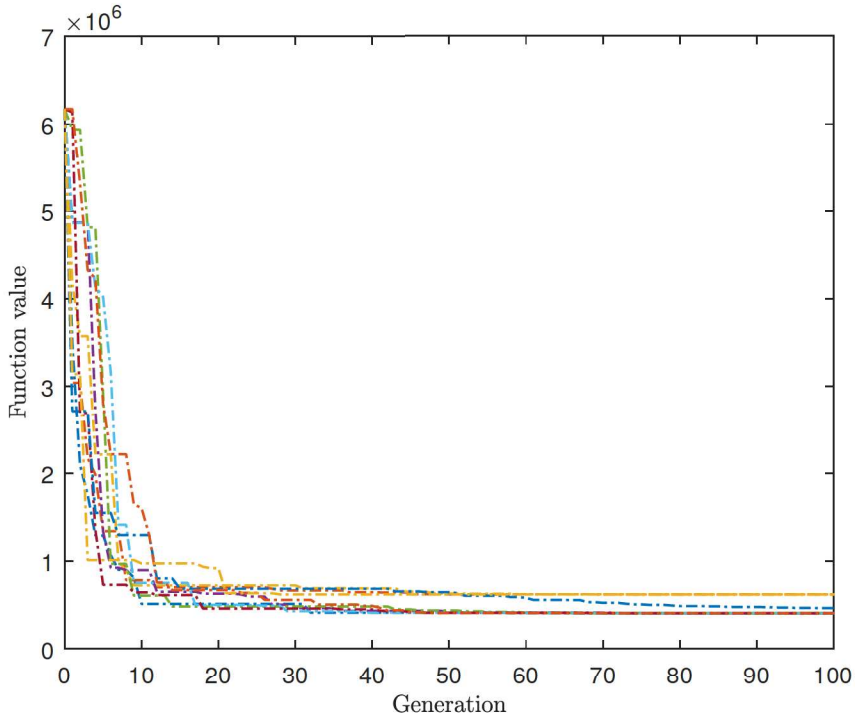


**Figure 6.14.** Convergence curves for Clustering using SA for 10 runs

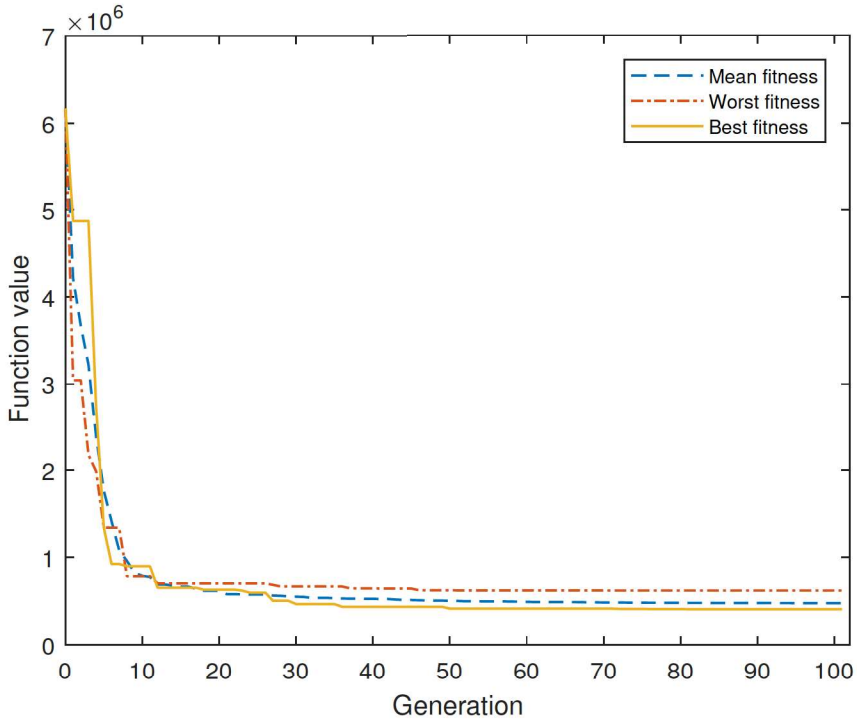


**Figure 6.15.** Best so-far curve for Clustering using SA

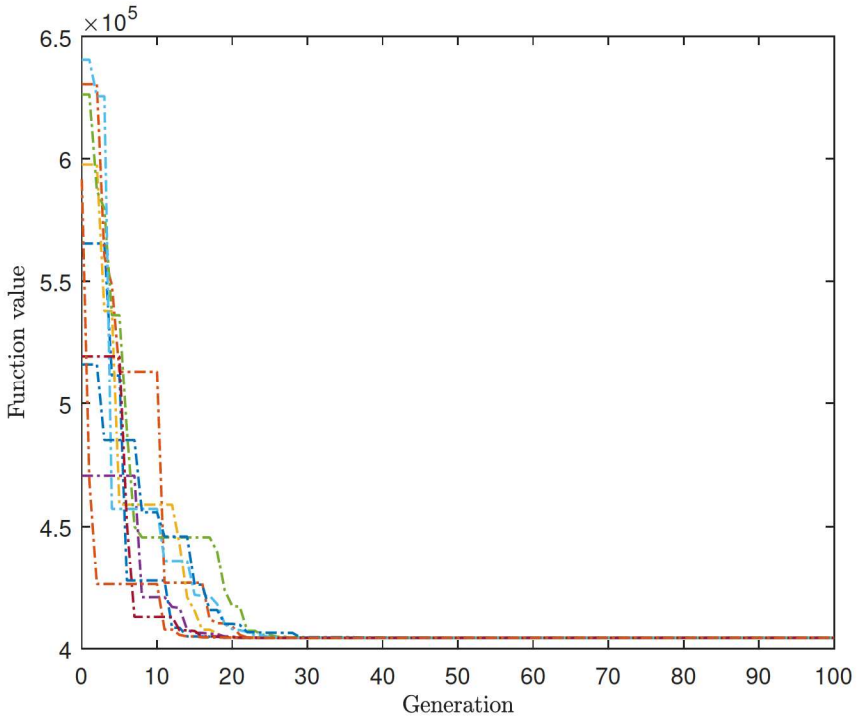


**Figure 6.16.** Convergence curves for Clustering using PSO for 10 runs

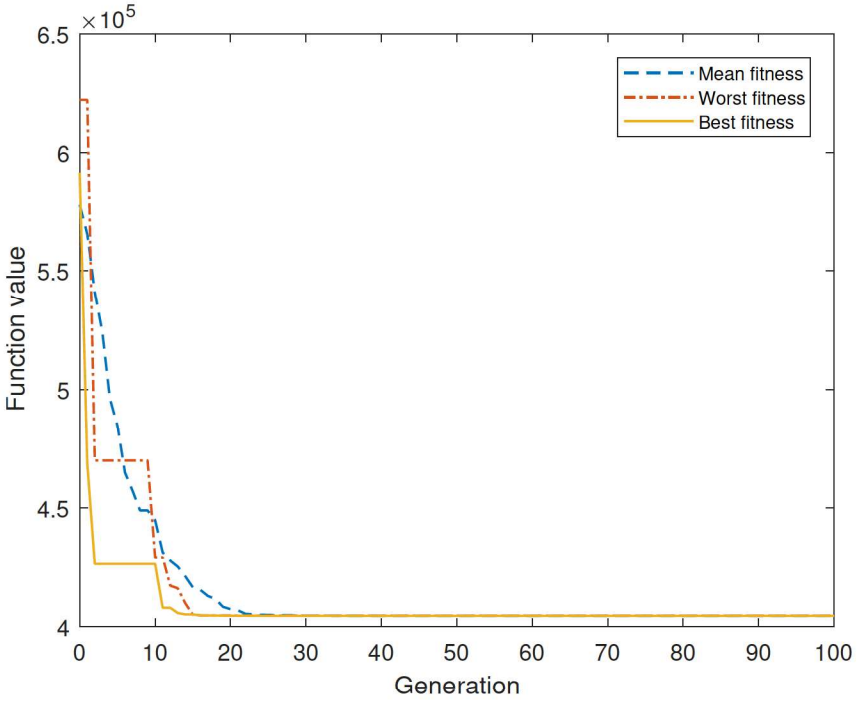


**Figure 6.17.** Best so-far curve for Clustering using PSO

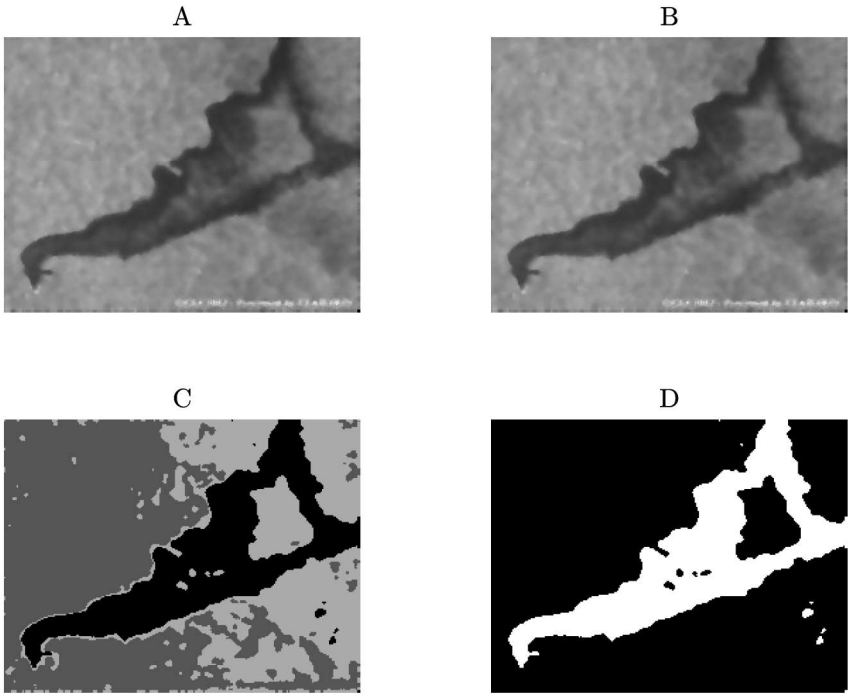


**Figure 6.18.** Thresholding based GA (A): Original image (B): Pre-processed image (C): Segmented image (D): Oil extracted image

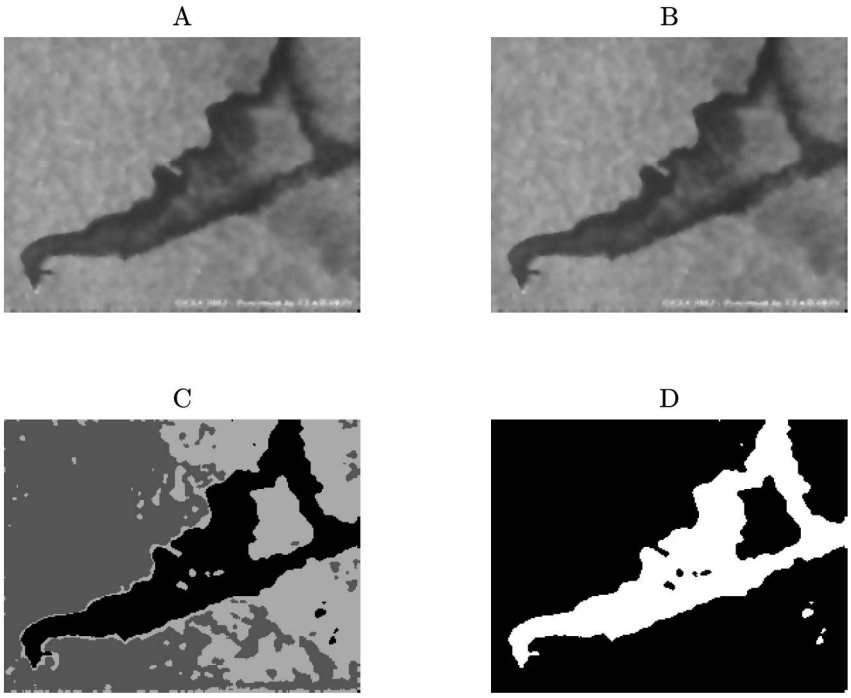


**Figure 6.19.** Thresholding based SA (A): Original image (B): Pre-processed image (C): Segmented image (D): Oil extracted image

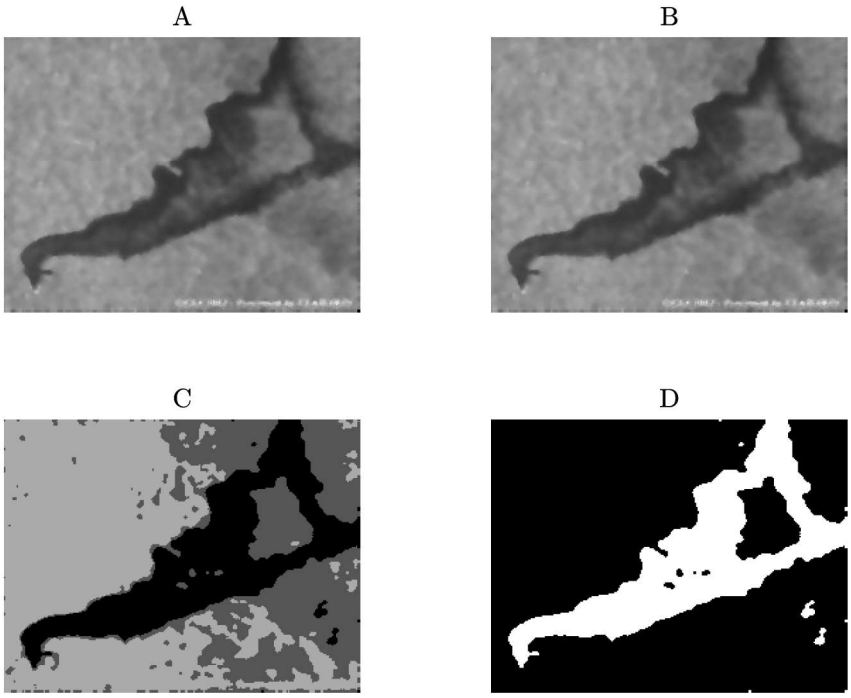


**Figure 6.20.** Thresholding based PSO (A): Original image (B): Pre-processed image (C): Segmented image (D): Oil extracted image

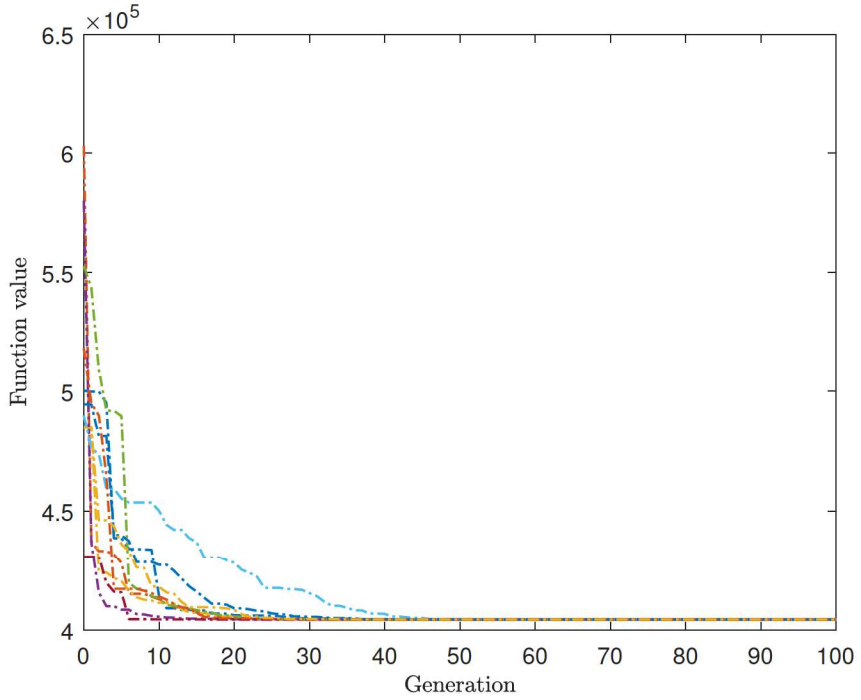


**Figure 6.21.** Convergence curves for Otsu based GA for 10 runs

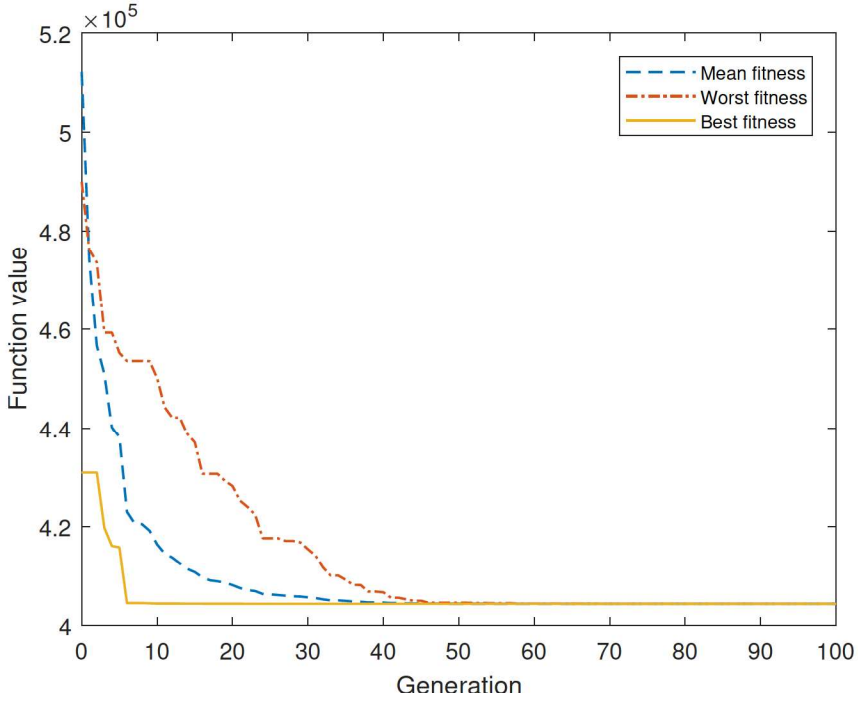


**Figure 6.22.** Best so-far curve for Otsu based GA

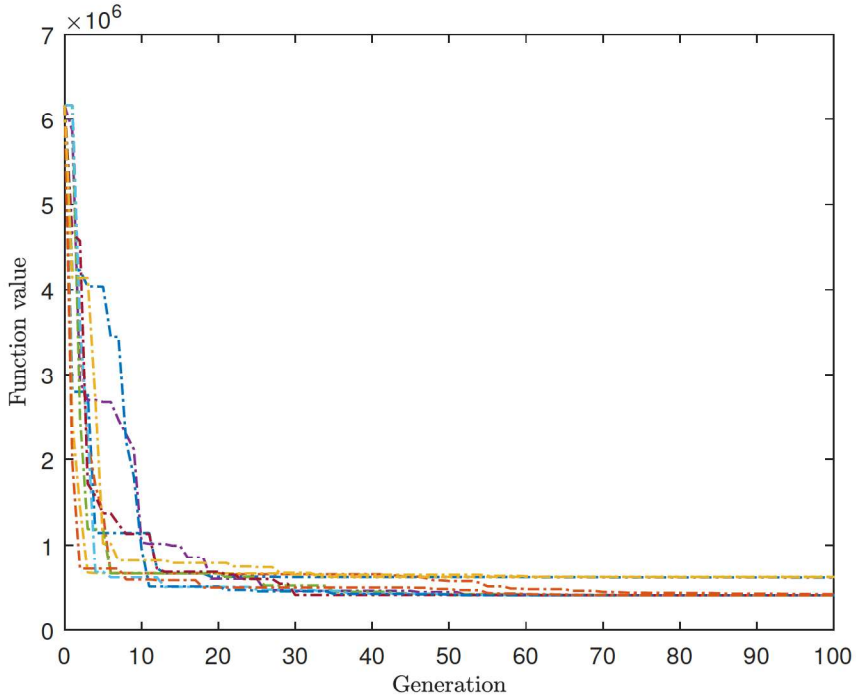


**Figure 6.23.** Convergence curves for Otsu based SA for 10 runs

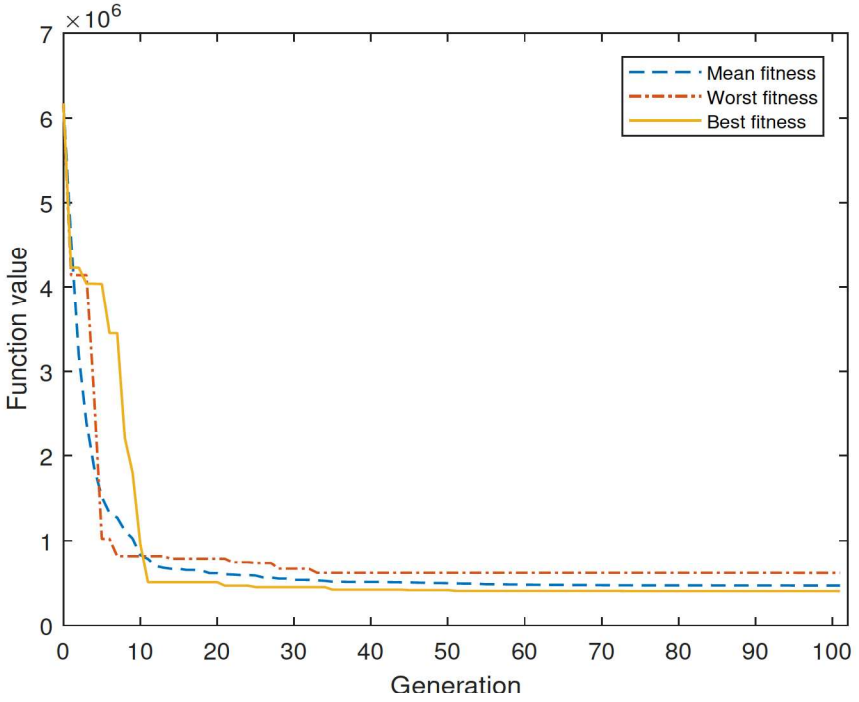


**Figure 6.24.** Best so-far curve for Otsu based SA

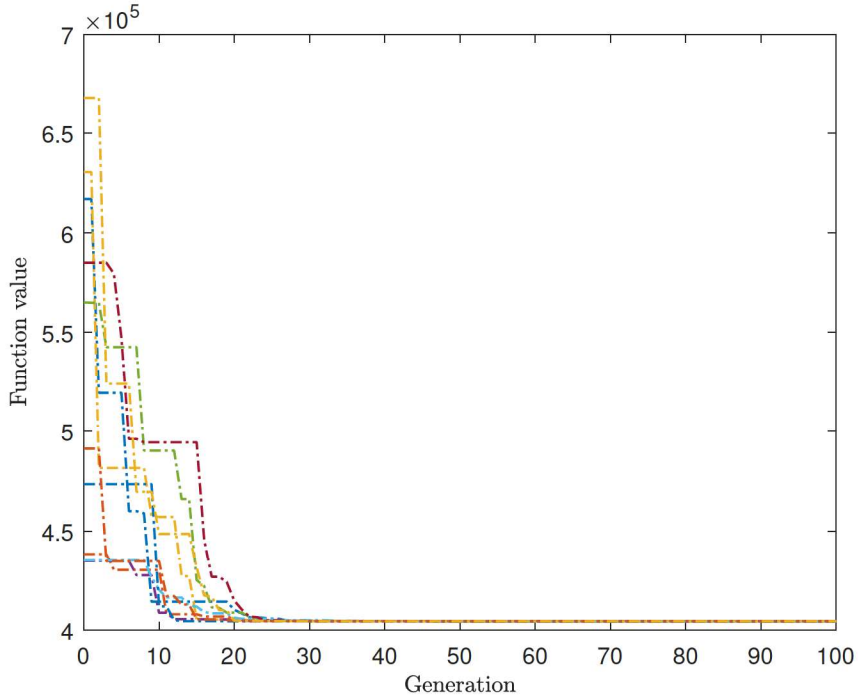


**Figure 6.25.** Convergence curves for Otsu based PSO for 10 runs

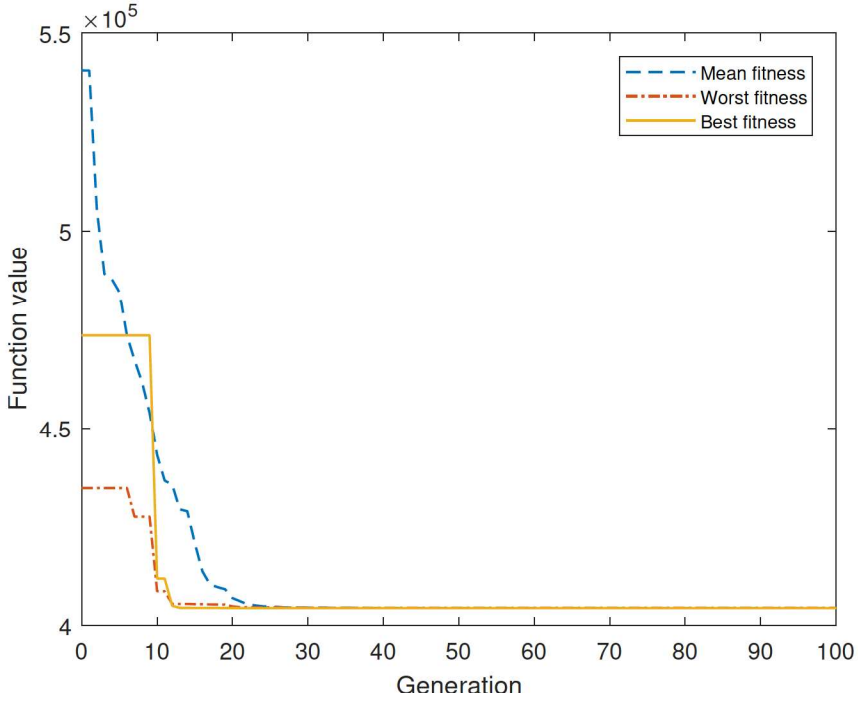


**Figure 6.26.** Best so-far curve for Otsu based PSO

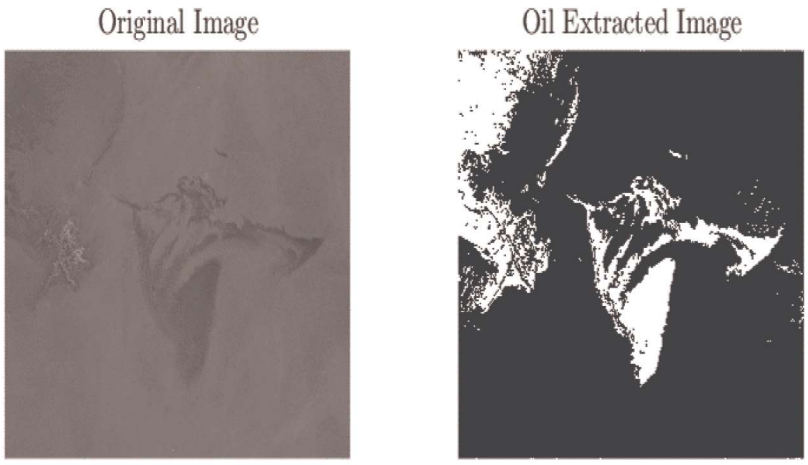


**Figure 6.27.** Database image 1

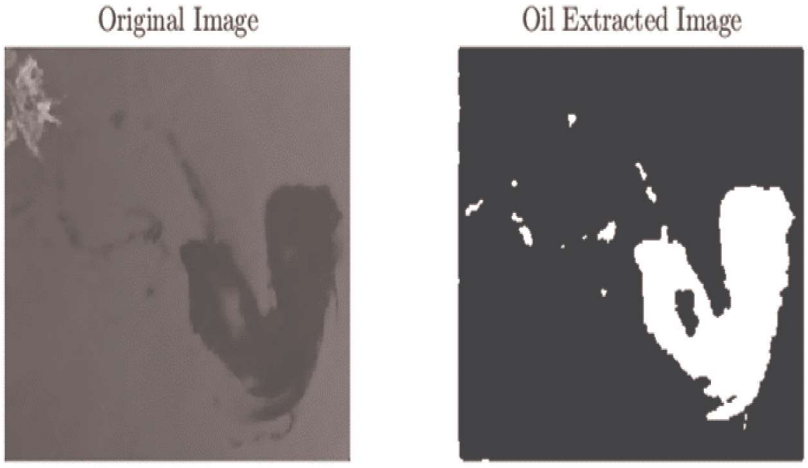


**Figure 6.28.** Database image 2

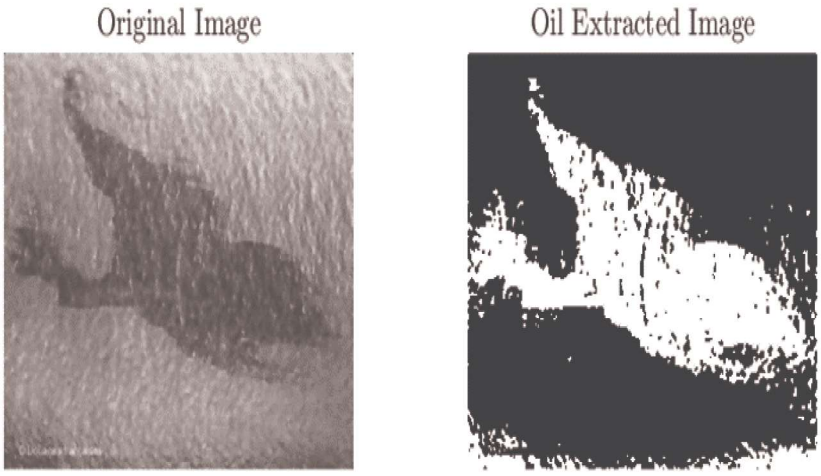


**Figure 6.29.** Database image 3

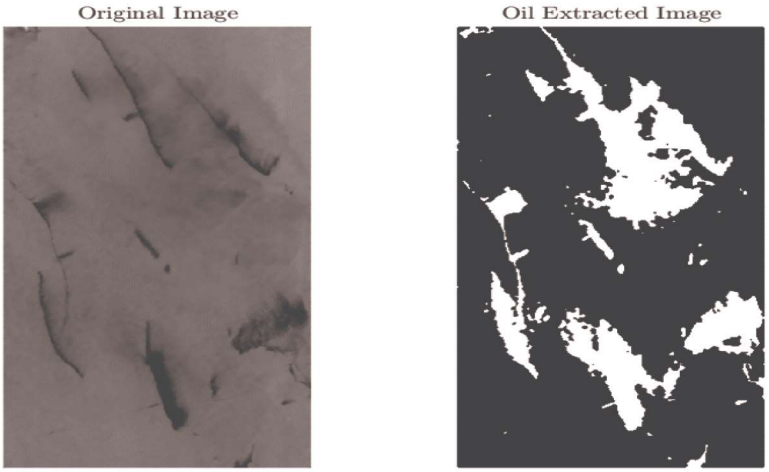


**Figure 6.30.** Database image 4

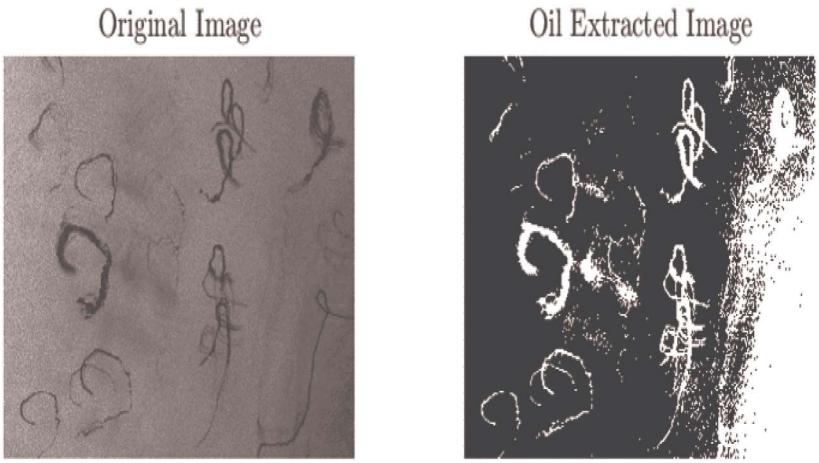


**Figure 6.31.** Database image 5

# CHAPTER 7

## CONCLUSION AND FUTURE WORK

Oil spills constitute a serious environmental and socio-economic problem. Oil spill detection is an important part of oil spill contingency planning. This work presents two frameworks for extracting oil from a SAR image using MHS. The MHS clustering algorithm has as objective to minimize the intra-cluster distances and maximize the inter-cluster distances. The Meta-heuristic search algorithms thresholding algorithm has an objective to minimize the intra-class variance. The proposed frameworks outperform the traditional methods of extracting the oil from SAR images. Three different Meta-heuristic search algorithms are used in this work for comparison GA, SA, and PSO. Based on the results obtained from the experiments PSO outperformed the other two Meta-heuristic search algorithms as well as traditional segmentation methods like K-means, FCM and Otsu methods. As result of a lot of noise present in SAR images, it is difficult to differentiate if the segmented object is either oil or look alike and also using multiple sensor technologies can improve the model.

## REFERENCES


[1] Allen, A. A. Contained controlled burning of spilled oil during the exxon valdez oil spill. *Spill Technology Newsletter 15*, 2 (1990), 1–5.

[2] Analoui, M. Radiographic image enhancement. part i: spatial domain techniques. *Dentomaxillofacial Radiology 30*, 1 (2001), 1–9.

[3] Bandyopadhyay, S., Maulik, U., and Pakhira, M. K. Clustering using simulated annealing with probabilistic redistribution. *International Journal of Pattern Recognition and Artificial Intelligence 15*, 02 (2001), 269–285.

[4] Baxes, G. A. *Digital image processing: principles and applications*. Wiley New York, 1994.

[5] Bhanu, B., Lee, S., and Ming, J. Adaptive image segmentation using a genetic algorithm. *IEEE Transactions on systems, man, and cybernetics 25*, 12 (1995), 1543–1567.

[6] Brieck, E. F. Oil spill skimmer, June 17 1980. US Patent 4,208,287.

[7] Camphuysen, C., and Heubeck, M. Marine oil pollution and beached bird surveys: the development of a sensitive monitoring instrument. *Environmental pollution 112*, 3 (2001), 443–461.

[8] Choi, H. M., and Cloud, R. M. Natural sorbents in oil spill cleanup. *Environmental science & technology 26*, 4 (1992), 772–776.

[9] Dunn, J. C. A fuzzy relative of the isodata process and its use in detecting compact well-separated clusters.

[10] Fay, J. A. The spread of oil slicks on a calm sea. In *Oil on the Sea*. Springer, 1969, pp. 53–63.

[11] Fingas, M., and Brown, C. Review of oil spill remote sensing. *Marine pollution bulletin 83*, 1 (2014), 9–23.

[12] Fingas, M. F., and Brown, C. E. Review of oil spill remote sensing. *Spill Science & Technology Bulletin 4*, 4 (1997), 199–208.

[13] Fiscella, B., Giancaspro, A., Nirchio, F., Pavese, P., and Trivero, P. Oil spill detection using marine sar images. *International Journal of Remote Sensing 21*, 18 (2000), 3561–3566.

[14] Hori, O. A video text extraction method for character recognition. In *Document Analysis and Recognition, 1999. ICDAR'99. Proceedings of the Fifth International Conference on* (1999), IEEE, pp. 25–28.

[15] Houck, C. R., Joines, J., and Kay, M. G. A genetic algorithm for function optimization: a matlab implementation. *Ncsu-ie tr 95*, 09 (1995), 1–10.

[16] Jha, D., Kim, J.-I., Choi, M.-R., and Kwon, G.-R. Pathological brain detection using weiner filtering, 2d-discrete wavelet transform, probabilistic pca, and random subspace ensemble classifier. *Computational intelligence and neuroscience 2017* (2017).

[17] Jha, M. N., Levy, J., and Gao, Y. Advances in remote sensing for oil spill disaster management: state-of-the-art sensors technology for oil spill surveillance. *Sensors 8*, 1 (2008), 236–255.

[18] Khashandarag, A. S., Mirnia, M., and Sakhavati, A. A new method for medical image clustering using genetic algorithm. *IJCSI International Journal of Computer Science Issues 10*, 1 (2013), 551–557.

[19] Khoshahval, F., Minuchehr, H., and Zolfaghari, A. Performance evaluation of pso and ga in pwr core loading pattern optimization. *Nuclear Engineering and Design 241*, 3 (2011), 799–808.

[20] Kirkpatrick, S., Gelatt, C. D., and Vecchi, M. P. Optimization by simulated annealing. *science 220*, 4598 (1983), 671–680.

[21] Kleindienst, S., Seidel, M., Ziervogel, K., Grim, S., Loftis, K., Harrison, S., Malkin, S. Y., Perkins, M. J., Field, J., Sogin, M. L., et al. Chemical dispersants can suppress the activity of natural oil-degrading microorganisms. *Proceedings of the National Academy of Sciences 112*, 48 (2015), 14900–14905.

[22] Lee, J.-S. Digital image enhancement and noise filtering by use of local statistics. *IEEE transactions on pattern analysis and machine intelligence*, 2 (1980), 165–168.

[23] Lehr, W. J. Review of modeling procedures for oil spill weathering behavior. *Advances in Ecological Sciences 9* (2001), 51–90.

[24] Liu, S., Chi, M., Zou, Y., Samat, A., Benediktsson, J. A., and Plaza, A. Oil spill detection via multitemporal optical remote sensing images: A change detection perspective. *IEEE Geoscience and Remote Sensing Letters 14*, 3 (2017), 324–328.

[25] Luke, B. T., et al. Simulated annealing cooling schedules. *http://members. aol. com/btluke/simanf1. htm, accessed June 1* (2007), 2007.

[26] MacQueen, J., et al. Some methods for classification and analysis of multivariate observations. In *Proceedings of the fifth Berkeley symposium on mathematical statistics and probability* (1967), vol. 1, Oakland, CA, USA, pp. 281–297.

[27] Maulik, U., Bandyopadhyay, S., and Pakhira, M. K. Clustering using annealing evolution: Application to pixel classification of satellite images. In *ICVGIP* (2002).

[28] Narasimhan, S. G., and Nayar, S. K. Contrast restoration of weather degraded images. *IEEE transactions on pattern analysis and machine intelligence 25*, 6 (2003), 713–724.

[29] Niharika, E., Adeeba, H., Krishna, A. S. R., and Yugander, P. K-means based noisy sar image segmentation using median filtering and otsu method. In *IoT and Application (ICIOT), 2017 International Conference on* (2017), IEEE, pp. 1–4.

[30] Pal, N. R., and Pal, S. K. A review on image segmentation techniques. *Pattern recognition 26*, 9 (1993), 1277–1294.

[31] Pappas, T. N. An adaptive clustering algorithm for image segmentation. *IEEE Transactions on signal processing 40*, 4 (1992), 901–914.

[32] Peizhuang, W. Pattern recognition with fuzzy objective function algorithms (james c. bezdek). *SIAM Review 25*, 3 (1983), 442.

[33] Peterson, C. H., Rice, S. D., Short, J. W., Esler, D., Bodkin, J. L., Ballachey, B. E., and Irons, D. B. Long-term ecosystem response to the exxon valdez oil spill. *Science 302*, 5653 (2003), 2082–2086.

[34] Prince, R., Lessard, R., and Clark, J. Bioremediation of marine oil spills. *Oil & gas science and technology 58*, 4 (2003), 463–468.

[35] Roy, A., Singha, J., Manam, L., and Laskar, R. H. Combination of adaptive vector median filter and weighted mean filter for removal of high-density impulse noise from colour images. *IET Image Processing 11*, 6 (2017), 352–361.

[36] Russ, J. C. *The image processing handbook*. CRC press, 2016.

[37] Vala, M. H. J., and Baxi, A. A review on otsu image segmentation algorithm. *International Journal of Advanced Research in Computer Engineering & Technology (IJARCET) 2*, 2 (2013), pp–387.

[38] Volckaert, F., Kayens, G., Schallier, R., and Jacques, T. Aerial surveillance of operational oil pollution in belgiums maritime zone of interest. *Marine Pollution Bulletin 40*, 11 (2000), 1051–1056.

[39] Ware, C. K. Oil containment boom, Dec. 3 1996. US Patent 5,580,185.